Degree of branching in poly(acrylic acid) prepared by controlled and conventional radical polymerization

Alison Maniego, Adam Sutton, Yohann Guillaneuf, Catherine Lefay, Mathias Destarac, Christopher Fellows, Patrice Castignolles, Marianne Gaborieau

Polymer Chemistry

PAPER

Degree of branching in poly(acrylic acid) prepared by controlled and conventional radical polymerization

.Received 00th January 20xx,
Accepted 00th January 20xx

DOI: 10.1039/x0xx00000x

www.rsc.org/

Alison R. Maniego,[a,b] Adam T. Sutton,[a-c] Yohann Guillaneuf,[d] Catherine Lefay,[d] Mathias Destarac,[e] Christopher M. Fellows,[f] Patrice Castignolles,[*b] Marianne Gaborieau[a,b]

Poly(acrylic acid)s, PAAs and poly(sodium acrylate)s, PNaAs were characterized in detail. M_n was determined using size-exclusion chromatography, ^{1}H and ^{13}C NMR spectroscopy. There is no agreement between the results from different methods, possibly due to the surprisingly low solubility of PAA/PNaA in usual solvents such as dioxane, DMSO, and water. Clustering in PAA/PNaA (due to branching) should affect the molar mass determination by SEC and NMR spectroscopy differently. The degree of branching (*DB*) of PAAs and PNaAs obtained by reversible-deactivation radical polymerization (RDRP) and conventional radical polymerization (CVRP) was quantified by ^{13}C NMR spectroscopy. Previous investigations indicated that *DB* in poly(*n*-butyl acrylate) is lower when synthesized by RDRP than when synthesized by CVRP (without chain transfer agent, CTA). In the present work no substantial differences in *DB* were observed between PAAs synthesized via RDRP and CVRP in otherwise similar conditions of solvent and temperature. We believe that further investigations are necessary to know whether there are substantial differences in *DB* between poly(*n*-butyl acrylate)s synthesized by RDRP and the ones synthesized by CVRP or not. The *DB* values are higher for PAAs synthesized in dioxane than for PAAs/PNaAs synthesized in water, and adding ethanol to water further lowers the *DB* values. H-bonding of ethanol with PAA/PNaA or patching of the mid-chain radical by ethanol can lead to the decrease in *DB*. The polymerization conditions, polymerization temperature but also solvent, thus allow some tailoring of *DB* values depending on desired applications. The present manuscript provides an extended, reliable set of experimental data for PAA looking at the influence of polymerization process (controlled versus conventional), temperature, and solvent on *DB*. This will form a valuable basis for meaningful further in-depth kinetic investigations.

Introduction

Poly(acrylic acid) (PAA), or its salt form, poly(sodium acrylate) (PNaA), is a synthetic polymer used in sanitary products[1], water purification[2], drug delivery[3-5] and as an antiscaling agent [6-9]. The term "PAA/PNaA" is used here to refer to polymers that could be PAA (non-ionized PAA), PNaA (fully ionized PAA) or a copolymer of them (partially ionized PAA). In a similar way, the term "AA/NaA" is used to refer to acrylic acid monomers that could be non-ionized (AA), fully ionized (PNaA) or a mixture of both. The branching in PAA/PNaA is often overlooked as it is not introduced by design but rather by side reactions. Inter- and intramolecular (chain) transfer to poly(alkyl acrylates) results in a mid-chain radical (MCR) leading to branching (quaternary carbon).[10, 11] The same side reactions occur for the polymerization of AA/NaA. Branching has been identified using ^{13}C nuclear magnetic resonance (NMR) spectroscopy of PAA/PNaA obtained by radical polymerization.[12-17] The relation between polymerization conditions and the branching structures is however not well established.

The average degree of branching (*DB*) for poly(*n*-butyl acrylates) (PnBAs) obtained by conventional radical polymerization (CVRP) and reversible-deactivation radical polymerization (RDRP) including nitroxide mediated polymerization (NMP), reversible addition/fragmentation chain transfer (RAFT) and atom-transfer radical polymerization (ATRP) was investigated using solution-state ^{13}C NMR spectroscopy.[18] It was concluded that *DBs* in PnBAs obtained by CVRP were higher than in PnBAs obtained by RDRP methods. In this seminal work, no evidence was given that the difference in *DB* for PnBAs obtained by CVRP and RDRP was significant (see Figure S16). The reduction in *DB* has been elegantly rationalized considering competitive equilibria.[19] Two possible reasons were proposed for the reported reduction of

[a] Western Sydney University (WSU), Medical Sciences Research Group (MSRG), School of Science and Health (SSH), Parramatta, Australia.
[b] WSU, Australian Centre for Research on Separation Sciences (ACROSS), SSH, Parramatta, Australia, Email: p.castignolles@westernsydney.edu.au.
[c] University of South Australia, Future Industries Institute (FII), Mawson Lakes, Australia
[d] Aix Marseille Univ, CNRS, Institut de Chimie Radicalaire UMR 7273, Marseille, France
[e] Paul Sabatier University, Toulouse, France
[f] University of New England, Armidale, Australia
† Footnotes relating to the title and/or authors should appear here.
Electronic Supplementary Information (ESI) available: polymerization conditions, NMR conditions and spectra and related signal assignment as well as the equations to determine branching. See DOI: 10.1039/x0xx00000x

DB in PnBA in RDRP (ATRP[20] and NMP[21]). One theory suggests that the rate of intramolecular transfer is reduced in RDRP methods such as RAFT relative to CVRP[22] due to the short lifetime of the propagating radical in each propagation step.[23] The other theory suggests that patching of the MCR occurs (in the case of ATRP) and prevents it from undergoing side reactions leading to branching or β-scission.[24] In the case of NMP, the structure of the nitroxides used in the literature makes patching highly unlikely since the recombination of these nitroxides with a tertiary radical is much slower than the dissociation.[25] This controversy is not solved yet despite a large number of publications in the last years.[26] *DB* values in PAA/PNaA obtained by RDRP and CVRP have not yet been compared as far as we are aware and this is the main goal of this manuscript.

Other experimental conditions can also lead to variations in *DB* including degree of conversion[27, 28], temperature[29] and solvent[30, 31]. The activation energy of the transfer to polymer reactions is higher than the activation energy of the propagation which led to a higher *DB* at higher temperatures for PnBA.[11, 29] In this work, PAA/PNaA were obtained at degrees of conversion between 31 % and 97 % at temperatures between 35 °C and 120 °C.

Current catalysts used in ATRP have shown selective reactivity with acrylic acid (AA) forming metal carboxylates by reacting with the metal complexes instead of polymerizing.[32] These metal carboxylates act as poor deactivators and thus as poor ATRP catalysts.[32] As a result, *t*-butyl acrylate (tBA) is commonly used as a monomer for ATRP of polyacrylates and is also chosen for the ATRP samples investigated in this work. PAA can be synthesized by NMP[13, 14, 33, 34] and RAFT[35]/ macromolecular design via the interchange of xanthates (MADIX)[9].

Molar mass is both an important functional property of polymers and a key to understand polymerization. Molar mass values of polyelectrolytes determined by SEC generally suffer from poor reproducibility[36, 37] and in case of PAA/PNaA molar masses determined by aqueous versus organic systems differed by a factor of 2.[38]

In this work, the number average molar mass (M_n) was determined using ^{13}C NMR spectroscopy. M_n values obtained by ^{13}C NMR spectroscopy were compared to other experimental M_n values obtained by the widely used size-exclusion chromatography (SEC) and ^{1}H NMR spectroscopy. The *DB* values of PAA/PNaA synthesized by CVRP and RDRP (NMP, ATRP and MADIX) were also determined using quantitative solution-state ^{13}C NMR spectroscopy, in the conditions established in [15]. The precision and accuracy of PAA/PNaA *DB* values were determined as previously established[15] to ascertain whether different *DB* values are substantially different or not.

Theoretical ($M_{n(th)}$) and experimental ($M_{n(ex)}$) molar masses were compared in order to investigate the most accurate depiction of M_n. Measurements of $M_{n(ex)}$ of PAA/PNaA are mostly obtained by SEC ($M_{n(SEC)}$) or ^{1}H NMR spectroscopy ($M_{n(1H\ NMR)}$) in the literature.[39, 40] For this work M_n was determined by ^{13}C NMR spectroscopy ($M_{n(13C\ NMR)}$) for all samples for which spectra are quantitative for both backbone and end-group signals. $M_{n(ex)}$ was higher than $M_{n(th)}$ for most samples with the exception of 8 samples (out of 25). The relative difference (*RD*) between $M_{n(ex)}$ and $M_{n(th)}$ was plotted against the average *DB* (Figure S19). *RD* was large for most PAAs/PNaAs, and did not show a significant dependence on the polymerization solvent. Solubility should play a role in the $M_{n(ex)}$ determination, as solubility in water was observed to decrease with degree of polymerization, e.g., for oligo(acrylic acid) produced by RAFT polymerization.[41] Six out of 15 PAAs/PNaAs were previously observed to exhibit poor solubility by NMR spectroscopy even though no turbidity or undissolved material was visually observed (only a linear PNaA obtained by anionic polymerization was fully water-soluble).[15] The poor solubility observed in organic and aqueous solvents, including at different pDs in D_2O, is attributed to either microgel formations or clustering, in agreement with clustering previously observed by small-angle neutron scattering (SANS) for PAA in various solvents [42]. Incomplete solubility affects the accuracy of the $M_{n(ex)}$ determination. SEC, ^{1}H and ^{13}C NMR spectroscopy of PAA/PNaA were performed in "solution", which means that the obtained $M_{n(ex)}$ only represent the soluble fraction and not the whole sample, which could lead to an underestimation or an overestimation of $M_{n(ex)}$. The error bars given on Figure 1 do not relate to the accuracy, as affected by solubility, but only to precision as derived from the sensitivity of the NMR measurement. The sensitivity of ^{13}C NMR is lower than that of ^{1}H NMR. The errors bars are indeed larger for ^{13}C NMR results than ^{1}H NMR results. The error bars are however small compared to the accuracy (reproducibility) of the measured M_n values.

All samples presented in this work are branched (see next section). The presence of branching leads to a reduction in accuracy of M_n determination for PAA/PNaA via SEC.[38] Molar masses determined by organic-phase SEC may be less accurate than the ones determined by aqueous-phase SEC.[38] M_n values were determined using organic-phase SEC for the NMP and ATRP samples in this work. The $M_{n(SEC)}$ values obtained by organic-phase and aqueous-phase SEC were typically higher than $M_{n(th)}$ ones (Figure 1). Molar masses determined by different SEC methods (universal calibration with viscometer, MALLS) are also expected to be different for branched samples.[43] The heterogeneity of branching of these PNaAs could be determined by multiple detection SEC as it was done for poly(alkyl acrylates)[43] or by capillary electrophoresis in the critical conditions (CE-CC) as it was done for PAA/PNaA. [17, 44]

Results and discussion

Reproducibility of M_n values

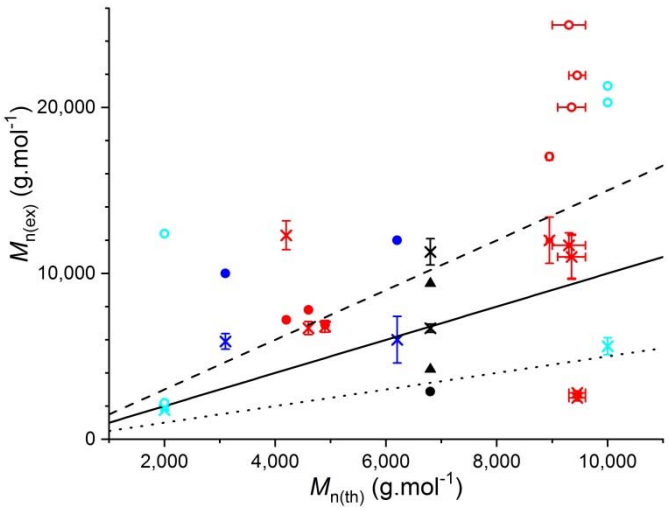

Figure 1. Comparison of $M_{n(th)}$ with $M_{n(ex)}$ determined for PAAs/PNaAs synthesized in dioxane using ^{13}C (×) NMR spectroscopy or organic-phase (●) and aqueous-phase (○) SEC, for PAAs/PNaAs synthesized in bulk using ^{1}H (▲) and ^{13}C (✕) NMR spectroscopy or organic-phase SEC (●),for PAAs/PNaAs synthesized in water/ethanol using ^{13}C NMR spectroscopy (×) or aqueous-phase SEC (○), for PAAs/PNaAs synthesized in water using ^{13}C NMR spectroscopy (×) or organic-phase SEC (●). The error bars are based on the precision estimated from the sensitivity of the NMR measurement (Y error bars) or the uncertainty on some kinetic parameters (X error bars). —— is the diagonal ($M_{n(th)}$=$M_{n(ex)}$), – – represents when $M_{n(th)}$ was 50 % lower than $M_{n(ex)}$, and ····· represents when $M_{n(ex)}$ was 50 % lower than $M_{n(th)}$. A larger version of this figure, with labels next to the data points indicating the sample codes (Figure S15), and a Table listing the plotted data (Table S9) are shown in supporting information.

Incomplete solubility was observed via ^{1}H NMR spectroscopy for NMP-AA-5 and NMP-AA-6 in D_2O with NaOD.[15] Poor solubility can thus also be expected for the MADIX samples analyzed by aqueous-phase SEC (Figure 1, empty red and light blue circles), leading to incorrect $M_{n(SEC)}$ values.

$M_{n(1H\ NMR)}$ and $M_{n(13C\ NMR)}$ were determined under the assumption that the polymerization is 100 % living for RDRP. Errors are thus possible for the determination of $M_{n(1H\ NMR)}$ and $M_{n(13C\ NMR)}$ as 100 % livingness was not observed for the polymerizations of PAA/PNaA in this work. $M_{n(th)}$ obtained by NMP in dioxane was calculated using the relation derived previously[14] taking into account the transfer to dioxane. For MADIX-AA3 to -6 the calculation of $M_{n(th)}$ is given in supporting information with Equations S2 and S3. No terminal double bonds were detected by NMR (see Figure S20) except for the polymerization at the highest temperature (120 °C): it is thus assumed that termination is predominantly by combination as observed in [45] and β-scission takes place at 120 °C. For conventional samples, CVRP, $M_{n(th)}$ was determined using Mayo's equation and a transfer coefficient to dioxane of 6 × 10^{-4}.[14] Different types of $M_{n(ex)}$ obtained by SEC, ^{1}H and ^{13}C NMR were thus compared to depict the most accurate representation of M_n (Figure 1). No single experimental method can be confirmed as the best method for the determination of $M_{n(ex)}$ due to their respective limitations. This confirms that M_n may be the most challenging polymer characteristics to accurately determine.[36]

Relation between polymerization conditions and average *DB*

Intra- and intermolecular (chain) transfer to polymer reactions during polymerization of AA/NaA and tBA lead to branching. The *DB*s were quantified in this work using ^{13}C NMR spectroscopy (Table S11, Figure 2) with the exception of samples NMP-tBA-1 and ATRP-tBA-3 for which there were issue with signal identification (Figure S9 and S10). The precision and accuracy of *DB* quantification has been assessed for numerous PAAs/PNaAs allowing the determination of error bars for the DB values reported in this work.[15]

The two parameters observed to have the largest influence on the average *DB* (Figure 2) are the solvent and polymerization temperature. The average *DB* increases with temperature [16, 17] as expected from the higher activation energy for transfer to polymer compared to propagation [11, 29, 46]. The average *DB* (at a given temperature) is substantially lower when the polymerization of AA (and/or its acrylate form) is performed in an aqueous solvent compared to an organic solvent (blue and red, respectively, on Figure 2). Only one monomer is present in organic solvents: AA. In water the monomers can be in both AA and its NaA conjugate forms in proportion varying with the pH. The lower *DB* observed in this work when some NaA is involved in the polymerization is consistent with the decrease in backbiting coefficient for NaA polymerization compared to that of AA.[47] In terms of polymerization rate AA has been observed to polymerize slower at a different rate compared to its conjugate base, with their polymerization rates depending also on factors such as pH, monomer concentration and counterion.[48, 49]

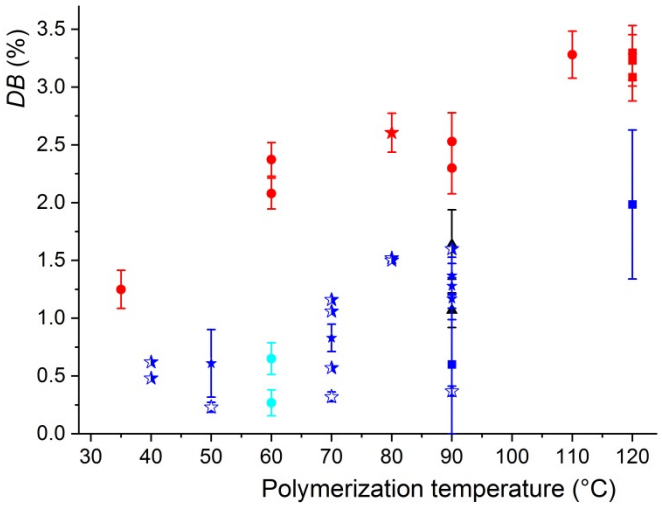

Figure 2. *DB* of PAAs/PNaAs synthesized in dioxane by NMP (■), MADIX (●) and CVRP (★), in bulk with ATRP (▲), in water/ethanol with MADIX (●), and in water with NMP (■), CVRP (★ from [16], ★ from [17]), and CVRP with CTA (☆ from [17]). The error bars are based on the precision estimated from the sensitivity of the NMR measurement. A larger version of this figure, with labels next to the data points indicating the sample codes (Figure S16), and a Table listing the plotted data (Table S11) are shown in supporting information

The type of synthesis, CVRP vs RDRP, does not substantially influence the average *DB*. In dioxane similar *DB* values were

determined for CVRP-AA-1 synthesized without chain transfer agent (Figure 2, red star) and the PAAs/PNaA synthesized by MADIX and NMP (taking the influence of temperature into account). In water, similar *DB* values were determined for a large number of PAA/PNaAs obtained by CVRP in the literature[16, 17] and our two PNaAs obtained via NMP in water (blue squares in Figure 2, taking the influence of temperature into account). For nBA, the prominence of short-chain radicals and the broad distribution of radical chain-length in CVRP in comparison to RDRP has been suggested to lead to a lower *DB* in RDRP.[18] Similar *DB*s were measured in the present work, within experimental error, for PAAs/PNaAs synthesized by RDRP and CVRP in the same solvent and at similar temperatures. The possible reasons for the reported lower *DB* of PnBA obtained by RDRP compared to PnBA obtained by CVRP seem to either not apply to PAA/PNaA, or to affect their *DB* only to a limited (non-detectable) extent. The precision and accuracy of the *DB* quantification in PnBAs[18] were not assessed with most *DB*s estimated in non-quantitative conditions (Figure S18). Moreover, some of the PnBAs investigated [18] were obtained in 50 % xylene rather than in bulk, thereby changing the polymerization solvent. Thus it may be asked whether the difference in *DB* observed for PnBAs obtained by CVRP and RDRP is substantial or within experimental error. A study similar to that of Maniego et al.[15] would be needed on the *DB* of PnBA to answer this question.

In the case of PAA/PNaA MCR patching by a control agent is not expected from the comparison of *DB* values, but measurements were made to see if such patching could be observed. Samples obtained by ATRP differ by their monomer: tBA and not AA or its conjugate base. Poly(nBA-*co*-*n*-butyl 2-bromoacrylate) obtained by ATRP was measured with ^{13}C NMR as a proof of concept that the mid-chain bromine C_q can be detected.[50] The ^{13}C NMR chemical shift of the OCH_2 group attached to the patched tertiary radical by the bromomonomer was measured at 66.4 ppm. For PAAs synthesized via ATRP in the present study ATRP-*t*BA-1 and 2 displayed insufficient resolution to rule out some patching with bromine as the patching signal overlaps with the solvent signal (see Figure S8 and S9 of [15]). The mid-chain bromine may also have already been eliminated during the hydrolysis step after the polymerization. Thus, the mechanism of MCR patching by bromine cannot be proven or disproven for ATRP-tBA-1 and 2. However, tBA (Figure 2, triangles) polymerized in bulk does not exhibit substantially different PAA/PNaA *DB* values compared to the direct polymerization of AA and its conjugate base in water.

Reduced *DB* has already been observed with PAA/PNaAs synthesized by CVRP with thioglycolic acid as a CTA in comparison to PAA/PNaAs without (Figure 2, blue empty and half-filled stars, respectively).[17] As noted above, two models have been proposed for the decreased *DB*: the short transient life of the propagating radical [22] or the patching of the MCR by the CTA which prevents branching[24, 29]. MADIX-AA-1 MADIX-AA-2 and MADIX-AA-4 were synthesized at the same temperature but in different solvents: ethanol and water for the first two (light blue circles in Figure 2) and dioxane (red circles in Figure 2, in duplicates) for the latter. MADIX-AA-1 and -2 exhibited very low *DB*s (Table S11) in comparison to MADIX-AA-4. There are two possible reasons for this. H-bonding between ethanol and PAA/PNaA may slow down the transfer to polymer, thus decreasing DB, similar to the model hypothesized for nBA [31] and 2-hydroxyethyl acrylate (EHA) polymerization in the presence of *n*-butanol.[30, 31, 51] The effect of *n*-butanol on EHA polymerization was however suppressed by *N*,*N*-dimethylformamide, a strong H-bonds acceptor. The effect of ethanol may thus also be suppressed by water, the main solvent in the synthesis of MADIX-AA-1 and -2. Patching of the MCR by the ethanol is the second possible reason for the decreased DB in MADIX-AA-1 and -2. Ethanol reacts with radical initiator leading to radical addition to olefins.[52, 53] Ethanol was also observed to inhibit radical photo-oxidation reactions in a reproducible fashion, even leading to a new method to quantify ethanol.[7] Transfer to ethanol was also used to explain a decrease in M_n in the presence of large amount of ethanol in the polymerization of ethylene[54], alkyl acrylates[55] and acrylamide[56] (transfer coefficients to ethanol were determined implicitly assuming no transfer to polymer[57] and no branching[58] and this would have an impact on the transfer coefficient values determined for ethylene and alkyl acrylates[55]). Abstraction of a hydrogen from the -CH_2- of the ethanol (and not from the –OH[52]) by the MCR is thus possible and can be the reason for the reduced DB in MADIX-AA-1 and -2.

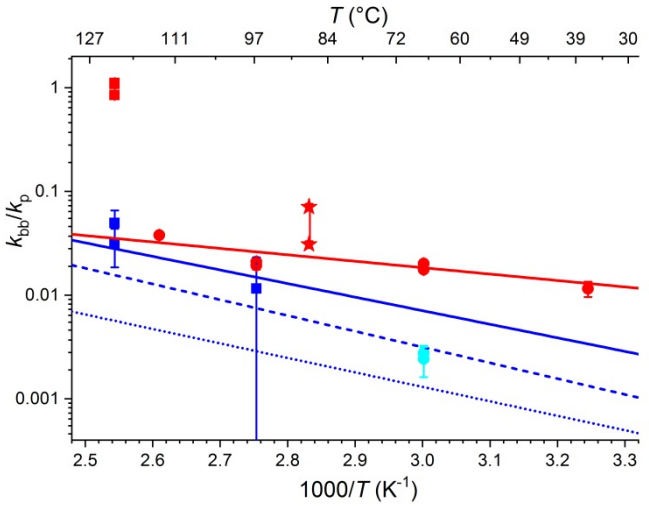

Figure 3. Arrhenius plot of k_{bb}/k_p for AA/NaA in dioxane by NMP (■), MADIX (●) and CVRP (★), in water with NMP (■), and in water/ethanol with MADIX (●).The error bars are based on the precision estimated from the sensitivity of the NMR measurement. The vertical bar linking the red stars represents the large uncertainty on the monomer conversion for sample CVRP-AA-1. —— represents the Arrhenius fit for MADIX in 1,4-dioxane-d_8 (ln y = -1425x + 0.28). – – and ····· represent Arrhenius fits from previous studies with CVRP in water: with and without CTA [17] (ln y = -3213x +2.998 and ln y = -3502x +4.747, respectively) and without CTA [16] (solid line, ln y = -3012x + 4.086). A larger version of this figure, with labels next to the data points indicating the sample codes (Figure S18), and a Table listing the plotted data (Table S12) are shown in supporting information

Rate coefficients of intramolecular transfer to polymer

Ratios of the rate coefficients of intramolecular transfer to polymer to propagation, k_{bb}/k_p, were estimated for CVRP of AA/NaA using previously determined *DB*.[16, 17] The assumptions must be made that every transfer to polymer event leads to branching and that the incidence of the following events may be disregarded: MCR patching, *β*-scission and termination by disproportionation, as well as monomer consumption via addition to MCR. In this work k_{bb}/k_p was estimated from *DB* for PAA/PNaAs synthesized by MADIX CVRP, and NMP using equation S29, taking the initial and final monomer concentrations into account (see supporting information).[59] For MADIX samples k_{bb}/k_p follows an apparent Arrhenius plot (Figure 3, red circles and red line) which was compared to corresponding Arrhenius plots of PAA/PNaAs synthesized via CVRP with or without CTA.[16, 17] The NMP in dioxane behaved differently to MADIX and CVRP in dioxane (red squares vs red circles and stars). This may be explained by the occurrence of appreciable β-scission for NMP in dioxane at 120 °C, making the assumptions done here to estimate k_{bb}/k_p from *DB* invalid. It is not the case for the NMP in water. This is consistent with ^{1}H NMR observations of terminal double bonds from β-scission observed for PAA obtained by NMP in dioxane but not by NMP in water.

While transfers to polymer are typically unwanted side reactions their combination with β-scission at high polymerization temperature has been used to produce macromonomers.[60, 61] Moreover, β-scission of the MCR can reduce branching due to the formation of a macromonomer. The macromonomer signals overlaps with the residual monomer ones (granted the latter is present) in ^{1}H NMR spectroscopy but can be differentiated through their different splitting patterns (Figure S20). The macromonomer signal was observed only in PAAs synthesized in dioxane at 120 °C (NMP-AA-1, NMP-AA-3 and NMP-AA-4). β-scission is thus taking place only at the highest temperature as was the case for poly(alkyl acrylates)[11, 61].

When β-scission is negligible, the polymerization process has no influence on the ratio k_{bb}/k_p of PAA/PNaA in a given solvent as confirmed when comparing NMP and CVRP in water (blue squares and solid blue line) or when comparing CVRP and MADIX in dioxane (red star and red circles). This confirms that the polymerization process does not substantially influence the formation of branches.

The ratio of pre-exponential factors A_{bb}/A_p was lower for MADIX in dioxane than for CVRP in water [16, 17] (Table 1). A lower difference in activation energies between intramolecular transfer to polymer and propagation ($E_{a,bb}$-$E_{a,p}$) was also observed for MADIX in dioxane than for CVRP in water [16, 17].

Table 1. Ratio of pre-exponentional factors A_{bb}/A_p and difference in activation energies $E_{a,bb}$-$E_{a,p}$ for the intramolecular transfer to polymer and propagation of AA in different polymerizations.

Polymerization process	A_{bb}/A_p	$E_{a,bb}$-$E_{a,p}$ (kJ·mol^{-1})
MADIX in dioxane	1.3	12
CVRP in water without CTA [16]	60	25
CVRP in water without CTA [17]	115	29
CVRP in water with CTA [17]	20	27

Conclusions

A variety of PAA/PNaAs obtained by RDRP and CVRP were characterized by ^{13}C NMR spectroscopy. A large discrepancy was observed between the experimental values of M_n obtained by SEC, ^{1}H and ^{13}C NMR. This issue may be due to the presence of branching and to the related low solubility of branched PAA/PNaAs. Dissolution of PAAs/PNaAs in their respective solvents of choice in their SEC and ^{1}H NMR spectroscopy analysis should be investigated in the future to provide insight on the reliability of their $M_{n(ex)}$ value. Despite the limitations of these methods, $M_{n(ex)}$ obtained by ^{13}C NMR spectroscopy should provide a more accurate $M_{n(ex)}$ value than ^{1}H NMR due to better resolution of signals, but with a much more limited throughput. When *DB* is measured and long ^{13}C NMR measurements are needed, then our recommendation is to take the opportunity to measure M_n by ^{13}C NMR as well.

The average *DB*s of different PAA/PNaAs synthesized by conventional and several RDRP methods were compared in this study. The expected increase in *DB* with temperature was confirmed experimentally. Lower *DB* values were observed for polymerization in water compared to dioxane. In a given solvent, RDRP and CVRP of AA/NaA led to similar *DB*s within experimental error. This situation seems to differ from the reported case of nBA.[18] As both the susceptibility of MCR to patching and the relative lifetime of the propagating secondary radicals should be similar for PAA/PNaA and PnBA, this casts doubt on both of the main explanations offered for

the difference between RDRP and CVRP reported for PnBA. We propose a systematic re-examination of the nBA results along the lines of the work reported here and in reference [15] (quantify solubility to assess accuracy, quantify precision from NMR spectrum signal-to-noise ratio) in order to determine whether the *DB*s are substantially different or within experimental error for PnBAs obtained by RDRP and CVRP.

The presence of CTA, but also of ethanol in CVRP reduces the *DB* values and this is most likely due to patching of the mid-chain radical. No macromonomers (from β-scission) were detected except at the highest polymerization temperature of 120 °C.

The large set of reliable, experimental *DB* values provided for PAA/PNaAs obtained by RDRP and CVRP in various solvents at various temperatures will enable further in-depth investigations of the complex polymerization kinetics of this family of monomers. It will also inform comprehensive approaches to tailor designs for specific applications. When one wishes a high *DB* value, e.g., for controlled drug release [5], then polymerization in dioxane at relatively high temperature should be favored. When one wishes a low *DB* value, e.g., for flocculation [2], then polymerization in water at relatively low temperature with some ethanol (or a very small amount of patching agent not limiting the molar mass) should be favored.

Experimental

Materials

Water was of Milli-Q quality. All deuterated solvents were as described in our previous work[15]

Polymerization

Sample codes and polymerization conditions are listed in Table S1. Polymerizations of samples were described in earlier publications for NMP[13] (universal calibration for samples NMP-AA-3 to -6), ATRP[8], MADIX[62], and conventional polymerization without chain transfer agent[13]. Additional information is given below Table S1 for samplesMADIX-AA-3 to 6 and the SEC of all samples. Conventional polymerization of AA with dodecanethiol as chain transfer agent was initiated with AIBN at 60 °C in toluene and DMF.

NMR spectroscopy

The instrumental parameters for one-dimensional[15] and two-dimensional[63] NMR were described in accompanying publications. One-dimensional NMR conditions like the concentration, number of scans, repetition delay, solvent were described in earlier work[15] but also summarized with the information for additional samples in the Supporting Information (Table S2). The assignment of chemical shifts for ^{1}H and ^{13}C NMR of PAA/PNaA is shown in the Supporting Information (Table S3 – S5, Figure S1 - S14) or in previous work[15].

DB quantification

DB in PAA/PNaAs was determined for most of the samples previously[15] with the exception of NMP-AA-4, NMP-AA-6, and MADIX-AA-1 to -3. *DB* values for NMP-AA-4 and MADIX-AA-1-3 were quantified in this work (Equation S25-S26, Table S9) whilst a maximal possible *DB* value for NMP-AA-6 was estimated using a 1-point calibration (explained in Supporting Information, Figure S17).

M_n quantification

M_n is defined as the total mass of polymer chains divided by the total number of chains. In NMR spectroscopy, monomer unit signals correspond to the total mass of polymer chains whilst end groups signals correspond to the total number of polymer chains. M_n can be determined from ^{13}C NMR spectroscopy as:

$$M_n = \frac{I(\mathrm{CH_2 + CH + C_q + } x\mathrm{C_{OL\ with\ end\ group}}) - xI(\mathrm{C_{end\ group}})}{2 \times I(\mathrm{C_{end\ group}})} \times M_\mathrm{m} \quad (1)$$

or:

$$M_n = \frac{I(\mathrm{C{=}O} + x\mathrm{C_{OL\ with\ end\ group}}) - xI(\mathrm{C_{end\ group}})}{I(\mathrm{C_{end\ group}})} \times M_\mathrm{m} \quad (2)$$

where *I* is the integral of the signals described in the following brackets, *x* is the number of end group signals overlapping with the backbone, M_m is the molar mass of the monomer unit, CH, CH_2 and C=O are signals from the monomer unit. Overlapping signals with the backbone like the branching point (C_q) and some end group signals were also taken into account. For this work, both approaches of equation 1 and 2 were followed (Table S6). Modified versions of Equation 1 and 2 specifically catered for every sample as shown in the Supporting Information (Equations S5-S24). *RSD* for the *DB* and M_n quantification were expressed in [15].

Conflicts of interest

There are no conflicts of interest to declare.

Acknowledgements

Many thanks to Prof. Greg Russell (University of Canterbury) and Dr Simon Harrisson (Federal University of Toulouse) for scientific discussions, as well as Dr Emmanuelle Read, Dr Ihor Kulai (Toulouse), Dr Ali Al-Hamzah, and Dr Christopher East (University of Sydney) for their contribution to the synthesis of the samples presented in this work. Thank you to Kevin P. Dizon and Matthew P. Van Leeuwen (WSU) for contributions to the calculations, Kash A. Bhullar (WSU) for his IT assistance and Jason Phan (WSU) for his experimental contribution (NMR). AM and AS thank the Australian Commonwealth Government for Australian Postgraduate Award (APA) and Research Training Program (RTP) scholarships, respectively. PC acknowledges WSU Academic Development Program to visit the Federal University of Toulouse.

Notes and references

1. S. Ratnapandian and S. B. Warner, *Tappi J.*, 1996, **79**, 173-177.
2. Y. Yu, R. G. Peng, C. Yang and Y. H. Tang, *J. Mater. Sci.*, 2015, **50**, 5799-5808.
3. Y. Dai, C. Zhang, Z. Cheng, P. A. Ma, C. Li, X. Kang, D. Yang and J. Lin, *Biomaterials*, 2012, **33**, 2583-2592.
4. Y. H. Huang, H. Q. Yu and C. B. Xiao, *Carbohydr. Polym.*, 2007, **69**, 774-783.
5. E. G. Whitty, Maniego, A. R., Bentwitch, S. A., Guillaneuf, Y., Jones, M. R., Gaborieau, M., Castignolles, P., *Macromol. Biosci.*, 2015, **15**, 1724-1734.
6. A. A. Al-Hamzah and C. M. Fellows, *Desalination*, 2015, **359**, 22-25.
7. J. D. Oliver, M. Gaborieau and P. Castignolles, *J. Chromatogr. A*, 2014, **1348**, 150-157.
8. A. D. Wallace, A. Al-Hamzah, C. P. East, W. O. S. Doherty and C. M. Fellows, *J. Appl. Polym. Sci.*, 2010, **116**, 1165-1171.
9. D. Taton, A. Z. Wilczewska and M. Destarac, *Macromol. Rapid Commun.*, 2001, **22**, 1497-1503.
10. M. Gaborieau, L. Nebhani, R. Graf, L. Barner and C. Barner-Kowollik, *Macromolecules*, 2010, **43**, 3868-3875.
11. T. Junkers and C. Barner-Kowollik, *J. Polym. Sci. A Polym. Chem.*, 2008, **46**, 7585-7605.
12. J. Loiseau, N. Doerr, J. M. Suau, J. B. Egraz, M. F. Llauro and C. Ladaviere, *Macromolecules*, 2003, **36**, 3066-3077.
13. A. R. Maniego, D. Ang, Y. Guillaneuf, C. Lefay, D. Gigmes, J. R. Aldrich-Wright, M. Gaborieau and P. Castignolles, *Anal. Bioanal. Chem.*, 2013, **405**, 9009-9020.
14. L. Couvreur, C. Lefay, J. Belleney, B. Charleux, O. Guerret and S. Magnet, *Macromolecules*, 2003, **36**, 8260-8267.
15. A. R. Maniego, A. T. Sutton, M. Gaborieau and P. Castignolles, *Macromolecules*, 2017, **50**, 9032–9041.
16. N. F. G. Wittenberg, C. Preusser, H. Kattner, M. Stach, I. Lacík, R. A. Hutchinson and M. Buback, *Macromol. React. Eng.*, 2015, **10**, 95-107.
17. J.-B. Lena, A. K. Goroncy, J. J. Thevarajah, A. R. Maniego, G. T. Russell, P. Castignolles and M. Gaborieau, *Polymer*, 2017, **114**, 209-220.
18. N. M. Ahmad, B. Charleux, C. Farcet, C. J. Ferguson, S. G. Gaynor, B. S. Hawkett, F. Heatley, B. Klumperman, D. Konkolewicz, P. A. Lovell, K. Matyjaszewski and R. Venkatesh, *Macromol. Rapid Commun.*, 2009, **30**, 2002-2021.
19. D. Konkolewicz, P. Krys and K. Matyjaszewski, *Accounts Chem. Res.*, 2014, **47**, 3028-3036.
20. N. Ballard, J. C. de la Cal and J. M. Asua, *Macromolecules*, 2015, **48**, 987-993.
21. N. Ballard, J. I. Santos and J. M. Asua, *Macromolecules*, 2015, **48**, 2909-2915.
22. Y. Reyes and J. M. Asua, *Macromol. Rapid Commun.*, 2011, **32**, 63-67.
23. N. Ballard, S. Rusconi, E. Akhmatskaya, D. Sokolovski, J. C. de la Cal and J. M. Asua, *Macromolecules*, 2014, **47**, 6580-6590.
24. D. Konkolewicz, S. Sosnowski, D. R. D'Hooge, R. Szymanski, M. F. Reyniers, G. B. Marin and K. Matyjaszewski, *Macromolecules*, 2011, **44**, 8361-8373.
25. J. Nicolas, E. Guegain and Y. Guillaneuf, in *Nitroxide Mediated Polymerization: From Fundamentals to Applications in Materials Science*, ed. D. Gigmes, Royal Society of Chemistry, Cambridge, 2016, pp. 305-348.
26. N. Ballard and J. M. Asua, *Prog. Polym. Sci.*, 2018, **79**, 40-60.
27. B. Wenn, G. Reekmans, P. Adriaensens and T. Junkers, *Macromol. Rapid Commun.*, 2015, **36**, 1479-1485.
28. P. A. Lovell, T. H. Shah and F. Heatley, in *Polymer latexes, Preparation, Characterization, Applications*, eds. E. S. Daniels, E. D. Sudol and M. S. El-Aasser, 1992, vol. 492, chap. 12, pp. 188-202.
29. M. Gaborieau, S. P. S. Koo, P. Castignolles, T. Junkers and C. Barner-Kowollik, *Macromolecules*, 2010, **43**, 5492–5495.
30. K. Liang and R. A. Hutchinson, *Macromol. Rapid Commun.*, 2011, **32**, 1090-1095.
31. K. Liang, R. A. Hutchinson, J. Barth, S. Samrock and M. Buback, *Macromolecules*, 2011, **44**, 5843-5845.
32. T. E. Patten and K. Matyjaszewski, *Adv. Mater.*, 1998, **10**, 901-915.
33. J. Nicolas, Y. Guillaneuf, C. Lefay, D. Bertin, D. Gigmes and B. Charleux, *Prog. Polym. Sci.*, 2013, **38**, 63-235.
34. C. Lefay, J. Belleney, B. Charleux, O. Guerret and S. Magnet, *Macromol. Rapid Commun.*, 2004, **25**, 1215-1220.
35. M. F. Llauro, J. Loiseau, F. Boisson, F. Delolme, C. Ladaviere and J. Claverie, *J. Polym. Sci. A Polym. Chem.*, 2004, **42**, 5439-5462.
36. D. Berek, *J. Sep. Sci.*, 2010, **33**, 315-335.
37. A. Ritter, M. Schmid and S. Affolter, *Polym. Test*, 2010, **29**, 945-952.
38. I. Lacík, M. Stach, P. Kasák, V. Semak, L. Uhelská, A. Chovancová, G. Reinhold, P. Kilz, G. Delaittre, B. Charleux, I. Chaduc, F. D'Agosto, M. Lansalot, M. Gaborieau, P. Castignolles, R. G. Gilbert, Z. Szablan, C. Barner-Kowollik, P. Hesse and M. Buback, *Macromol. Chem. Phys.*, 2015, **216**, 23-37.
39. T. Fukuda, *J. Polym. Sci. A Polym. Chem.*, 2004, **42**, 4743-4755.
40. F. A. Bovey and P. A. Mirau, in *NMR of Polymers*, Academic Press, San Diego, 1996, ch. 3, pp. 155-241.
41. P. Castignolles, M. Gaborieau, E. F. Hilder, E. Sprong, C. J. Ferguson and R. G. Gilbert, *Macromol. Rapid Commun.*, 2006, **27**, 42-46.
42. B. Hammouda, F. Horkay and M. L. Becker, *Macromolecules*, 2005, **38**, 2019-2021.
43. M. Gaborieau and P. Castignolles, *Anal. Bioanal. Chem.*, 2011, **399**, 1413-1423.
44. J. J. Thevarajah, Sutton, A. T., Maniego, A. R., Whitty, E. G., Cottet, H., Castignolles, P., Gaborieau, M., *Anal. Chem.*, 2016, **88**, 1674-1681.
45. R. J. Minari, G. Caceres, P. Mandelli, M. M. Yossen, M. Gonzalez-Sierra, J. R. Vega and L. M. Gugliotta, *Macromol. React. Eng.*, 2011, **5**, 223-231.
46. A. Agirre, J. I. Santos, A. Etxeberria, V. Sauerland and J. R. Leiza, *Polym. Chem.*, 2013, **4**, 2062-2079.
47. J. Barth and M. Buback, *Macromolecules*, 2012, **45**, 4152-4157.
48. S. Khanlari and M. A. Dube, *J. Macromol. Sci. A Pure Appl. Chem.*, 2015, **52**, 587-592.
49. P. Drawe, M. Buback and I. Lacik, *Macromol. Chem. Phys.*, 2015, **216**, 1333-1340.
50. N. Ballard, M. Salsamendi, J. I. Santos, F. Ruiperez, J. R. Leiza and J. M. Asua, *Macromolecules*, 2014, **47**, 964-972.
51. K. Liang and R. A. Hutchinson, *Macromol. Symp.*, 2013, **325**, 203-212.
52. Z.-Q. Liu, L. Sun, J.-G. Wang, J. Han, Y.-K. Zhao and B. Zhou, *Org. Lett.*, 2009, **11**, 1437-1439.
53. W. H. Urry, F. W. Stacey, E. S. Huyser and O. O. Juveland, *J. Am. Chem. Soc.*, 1954, **76**, 450-455.
54. G. A. Mortimer, *J Polym. Sci. A-1 Polym. Chem.*, 1966, **4**, 881-900.

55. U. S. Nandi, M. Singh and P. V. T. Raghuram, *Makromol. Chem.*, 1982, **183**, 1467-1472.
56. B. Grassl, A. M. Alb and W. F. Reed, *Macromol. Chem. Phys.*, 2001, **202**, 2518-2524.
57. A. N. Nikitin and R. A. Hutchinson, *Macromolecules*, 2005, **38**, 1581-1590.
58. P. Castignolles, *Macromol. Rapid Commun.*, 2009, **30**, 1995 - 2001.
59. A. N. Nikitin, R. A. Hutchinson, G. A. Kalfas, J. R. Richards and C. Bruni, *Macromol. Theory Simul.*, 2009, **18**, 247-258.
60. J. Chiefari, J. Jeffery, R. T. A. Mayadunne, G. Moad, E. Rizzardo and S. H. Thang, *Macromolecules*, 1999, **32**, 7700-7702.
61. A. M. Zorn, T. Junkers and C. Barner-Kowollik, *Macromol. Rapid Commun.*, 2009, **30**, 2028-2035.
62. A. T. Sutton, E. Read, A. R. Maniego, J. J. Thevarajah, J.-D. Marty, M. Destarac, M. Gaborieau and P. Castignolles, *J. Chromatogr. A*, 2014, **1372**, 187-195.
63. A. T. Sutton, R. D. Arrua, M. Gaborieau, P. Castignolles and E. F. Hilder, *Anal. Chim. Acta*, 2018, **1032**, 163-177.

Table of Contents entry

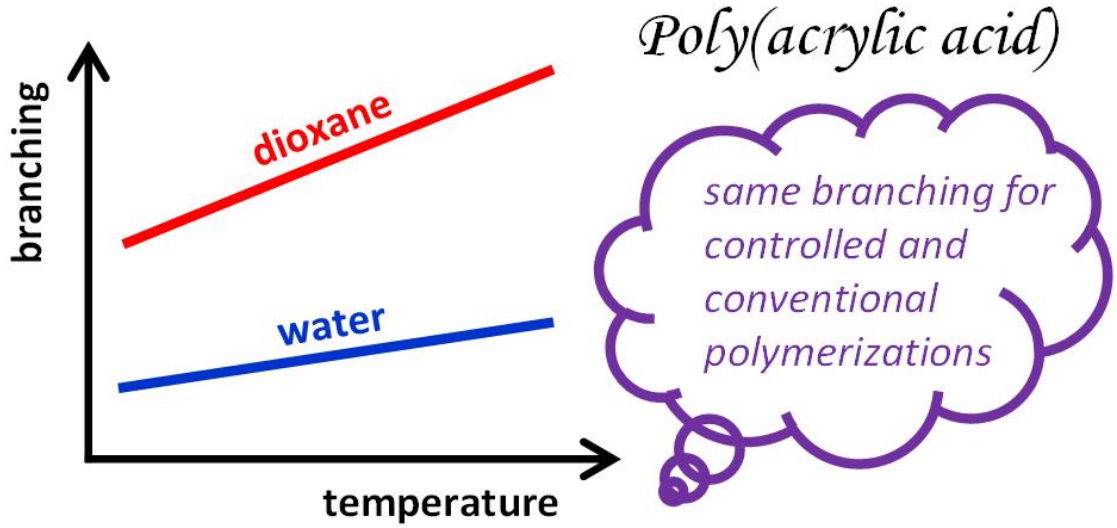

Supporting Information for

Degree of branching in poly(acrylic acid) prepared by controlled and conventional radical polymerization

Alison R. Maniego,[a, b] Adam T. Sutton,[a-c] Yohann Guillaneuf,[d] Catherine Lefay,[d] Mathias Destarac,[e] Christopher M. Fellows,[f] Patrice Castignolles,[*b] Marianne Gaborieau[a, b]

[a]Western Sydney University (WSU), Medical Sciences Research Group (MSRG), School of Science and Health (SSH), Parramatta, Australia

[b]WSU, Australian Centre for Research on Separation Science (ACROSS), SSH, Parramatta, Australia

[c]University of South Australia, Future Industries Institute (FII), Mawson Lakes, Australia

[d]Aix Marseille Univ, CNRS, Institut de Chimie Radicalaire UMR 7273, Marseille, France

[e]Paul Sabatier University, Toulouse, France

[f]University of New England, Armidale, Australia

*corresponding author: p.castignolles@westernsydney.edu.au

Polymerization conditions

In this work, PAAs and PNaAs were synthesized using CVRP, NMP, MADIX and ATRP methods. Polymerization conditions of AA and NaAs were as specified below.

Table S1. Description of PAAs/PNaAs investigated in this work. *T* stands for temperature, *x* for conversion. XA for 2-mercaptopropionic acid methyl ester O-ethyl dithiocarbonate, MONAMS for methyl 2-[*N*-*t*-butyl-*N*-(1-diethoxyphosphoryl-2,2-dimethylpropyl)aminoxy]propionate, BB for BlocBuilder, tBA for *t*-butyl acrylate, ACVA for 4,4'-azobis(4-cyanovaleric acid), ACD for 2,2'-azobis(4-methoxy-2.4-dimethyl valeronitrile), AIBN for 2,2'-azobisisobutyronitrile, ACBN for 1,1'-azobis(cyclohexanecarbonitrile), HB for hexyl 2-bromoisobutyrate, and HDB to hexadecyl-2-bromoisobutyrate, DMF for *N*,*N*-dimethylformamide, and n.d. for not determined. [a] Experimental parameters were chosen aiming at a theoretical M_n of 10,000 for 100 % conversion.

Sample code	***Synthesis***	***Control Agent (concentration)***	***Initiator (concentration, mM)***	***Monomer (concentration, M)***	***Solvent (volume, mL)***	***Time (h)***	***T (° C)***	***x (%)***
NMP-AA-1	NMP	SG1 (9 mol% with respect to MONAMS)	MONAMS (0.912)	AA (3.03)	1,4-Dioxane (35)	3	120	72
NMP-AA-3	NMP	SG1 (9 mol% with respect to MONAMS)	MONAMS [a]	AA (3)	1,4-Dioxane	3	120	63
NMP-AA-4	NMP	SG1 (9 mol% with respect to BB)	BB [a]	AA (3)	1,4-Dioxane	3	120	64
NMP-AA-5	NMP	SG1 (50 mol% with respect to BB)	BB [a]	AA (3)	Water, pH = 7	1	120	31
NMP-AA-6	NMP	SG1 (15 mol% with respect to BB)	BB [a]	AA (3)	Water, pH = 7	1	90	62

NMP-tBA-1	NMP of tBA, hydrolysis	SG1 (9 mol% with respect to MONAMS)	MONAMS (0.912)	tBA (3.03)	1,4-Dioxane (35)	3	120	65
MADIX-AA-1	MADIX	AX (136 mM)	ACVA (9.2)	AA (5.6)	Water (8) / ethanol (2)	4.5	60	99
MADIX-AA-2	MADIX	AX (22 mM)	ACVA (7.1×10^{-2})	AA (2.3)	Water (8) / ethanol (2)	4.5	60	99
MADIX-AA-3	MADIX	AX (22 mM)	ACD (2.2)	AA (3.03)	1,4-Dioxane (70)	15	35	95
MADIX-AA-4	MADIX	AX (22 mM)	AIBN (2.2)	AA (3.03)	1,4-Dioxane (70)	15	60	97
MADIX-AA-5	MADIX	AX (22 mM)	ACBN (2.2)	AA (3.03)	1,4-Dioxane (70)	15	90	97
MADIX-AA-6	MADIX	AX (22 mM)	*t*-Butyl peroxide (2.2)	AA (3.03)	1,4-Dioxane (70)	15	110	91
ATRP-tBA-1	ATRP of tBA, hydrolysis		HB (133)	tBA (6.8)	Bulk	>24	90	54
ATRP-tBA-2	ATRP of tBA, hydrolysis		HDB (134)	tBA (6.8)	Bulk	25	90	38
ATRP-tBA-3	ATRP of tBA, hydrolysis		HB (289)	tBA (6.8)	Bulk	>24	90	89
CVRP-AA-1 (CONV-AA-1 in [1])	Conventional		AIBN (26.1)	AA (3.03)	1,4-Dioxane (35)	3.5	120	n.d.

The synthesis of MADIX-AA-3 to MADIX-AA-6 was carried out in hermetic tubes equipped with a PTFE needle valve using 1,4-dioxane as solvent, AX as chain transfer agent and initiated with a series of thermal free radical initiators selected to have a half-life (5 to 38 h, see Table S7) much longer than the polymerization time. Acrylic acid (20 g, 0.278 mol, 3.03 mol L^{-1}), 1,4-dioxane (72.31 g) and AX (416.6 mg, 2 mmol, 21.86 mmol L^{-1}) were mixed together. 23.2 g of the obtained solution were placed in a tube with 0.05 mmol of the corresponding initiator, degassed with three freeze-pump-thaw cycles, sealed under vacuum and placed into a heating block with predefined temperature. After 15 h the tube was cooled, a sample was withdrawn to determine the conversion by ^{1}H NMR, and the polymerization mixture was precipitated twice into cold diethyl ether. The obtained residue was dried under reduced pressure to remove remaining organic solvents, dissolved in 100 mL of deionized water and freeze-dried, giving about 4 g of white solid (80 % recovery). The obtained polymers were analyzed by size-exclusion chromatography (SEC) on an Agilent 1100 HPLC system including a vacuum degasser and an isocratic pump monitored by an eclipse 2 system (Wyatt technology), a guard column Shodex SB-G and three columns Shodex OHpak in series (two SB-806 M HQ (8mm*300mm, 13µm) and one SB-802.5 HQ (8mm*300 mm, 6µm)) coupled with a refractometer (OptilabRex, Wyatt technology), a UV detector (Agilent) set at 290 nm and a multi-angle laser light scattering detector (Dawn HeleosII + QELS, 18 angles, Wyatt technology). The eluent used was an aqueous solution of NaCl (0.1 mol L^{-1}), NaH_2PO_4 (0.25 mmol L^{-1}) and Na_2HPO_4 (0.25 mmol L^{-1}). Prior to injections, samples were diluted to a concentration of 5 g L^{-1}, stirred overnight and filtered through 0.22µm Nylon filters. Values of M_n and $Đ$ are reported using SEC-MALS data. The dn/dc value (0.1457) was measured using a PSS DnDc-2010 differential refractometer (λ=620 nm, 35 °C).

SEC analysis of samples MADIX-AA-1 and -2 with universal calibration with a viscometer was carried out with a Malvern Triple Detector Array (TDA) SEC Model 305 with an online degasser, pump and a manual injector. They were eluted through one SEC SUPREMA pre-column (particle size of 5 µm) then through three SEC SUPREMA columns (two 1000 Å, particle size of 5 µm and one 30 Å, particle size of 5 µm) from Polymer Standards Service (PSS, Mainz) with an aqueous eluent containing 0.1 mol·L^{-1}, Na_2HPO_4 and 200 ppm NaN_3 at 50 °C and 1 mL·min^{-1} flow rate. The TDA includes the following detectors: right-angle laser light scattering (RALLS) and 7° low angle laser light scattering (LALLS) at 670 nm, refractometer and viscometer. Data was treated using OmniSEC version 4.7.0 and was plotted using OriginPro 8.5. Injections of PAA homopolymers and block copolymers used. All samples were filtered through a 0.45 µm PES or PVDF membrane filter before injection. The system was calibrated using 10 pullulan standards ranging from 342 to 708 000 g·mol^{-1} (molar mass at the peak) with dispersity inferior to 1.27. The obtained calibration curve was fitted with a 4th order polynomial: log M = 142.9 - 20.76x + 1.184x2 - 0.0301x3 + 0.0002824x4 (R^2=0.9994). Samples were injected at 8.17 g·L^{-1} for MADIX-AA-2 and 2.01 g·L^{-1} for MADIX-AA-1 with ethylene glycol as a flow rate marker.

SEC analysis of samples MADIX-AA-1 and -2 with MALLS detection was carried out on a system equipped with an on-line degasser, a Waters chromatography (Milford, MA) model 1515 isocratic pump, an autosampler (Waters 717), a refractometer (RI-101, Shodex)

thermostated at 25°C, a UV absorption detector (Prostar, Varian), refractive index detector (RI-101, Shodex) and a MALLS (Dawn Heleos, 18 angles, Wyatt Technology). The samples were eluted through a three-column set (8mm*300mm, 6µm particle size, 2* SB 806 M HQ columns and one SB 802.5 HQ protected by a guard column ShodexOHPak SB806-M) with an aqueous eluent containing 0.1 M $NaNO_3$ and 100 ppm NaN_3 at a flow rate of 1 $mL \cdot min^{-1}$. All samples were filtered through 0.45 µm membrane filter before injection. Samples were injected at ~ 5 $g \cdot L^{-1}$.

The SEC analysis was carried in THF after methylation for the samples synthesized by NMP and for sample CVRP-AA-1 [13] (with universal calibration for samples NMP-AA-1, NMP-AA-2, and CVRP-AA-1, and as PS-equivalent molar masses for samples NMP-AA-3 to 6), in THF for the PtBA precursors for samples synthesized by ATRP [8] (with calibration through M_n estimates from NMR), in 0.1 $mol \cdot L^{-1}$ Na_2HPO_4 in water for samples MADIX-AA-1 and MADIX-AA-2 [62].

References here have the same numbers as in the main manuscript:

Reference 8: A. D. Wallace, A. Al-Hamzah, C. P. East, W. O. S. Doherty and C. M. Fellows, *J. Appl. Polym. Sci.*, 2010, **116**, 1165-1171.

Reference 13: A. R. Maniego, D. Ang, Y. Guillaneuf, C. Lefay, D. Gigmes, J. R. Aldrich-Wright, M. Gaborieau and P. Castignolles, *Anal. Bioanal. Chem.*, 2013, **405**, 9009-9020.

Reference 62: A. T. Sutton, E. Read, A. R. Maniego, J. J. Thevarajah, J.-D. Marty, M. Destarac, M. Gaborieau and P. Castignolles, *J. Chromatogr. A*, 2014, **1372**, 187-195

^{13}C NMR conditions

Table S2. Experimental parameters for quantitative ^{13}C NMR experiments. All ^{13}C and ^{1}H NMR experiments were recorded at room temperature (25 °C).

Sample	***Solvent***	***Concentration ($g \cdot L^{-1}$)***	***Number of scans (NS)***	***Repetition delay (s)***	***DEPT-135 conducted (NS)***
NMP-AA-1	Dioxane-d_8	150	45,056	6.00	Yes (15,360)
NMP-AA-3	Dioxane-d_8	150	37,328	7.00	No
NMP-AA-4	Dioxane-d_8	150	49,152	8.00	Yes (14,794)
NMP-AA-5	D_2O / NaOD[a]	149	45,948	6.00	No
NMP-AA-6	D_2O / NaOD[a]	75	152,418	6.7	No
NMP-tBA-1	D_2O / NaOD [a] / DCl[b]	125	57,344	12.0[c]	Yes (36,272)
NMP-tBA-1	DMSO-d_6	69.9	27,653	6.00[c]	No
MADIX-AA-1	Dioxane-d_8	100	81,920	6.00	No
MADIX-AA-2	Dioxane-d_8	200	81,920	6.00	Yes (1,024)
MADIX-AA-3	Dioxane-d_8	200	32,768	10.0	Yes (24,155)
MADIX-AA-4	Dioxane-d_8	100	81,920	10.0	Yes (45,198)
MADIX-AA-5	Dioxane-d_8	200	16,774	10.0	Yes (22,770)
MADIX-AA-6	Dioxane-d_8	200	14,900	10.0	Yes (24,984)
ATRP-tBA-1	Dioxane-d_8	100	40,068	6.00	No
ATRP-tBA-2	Dioxane-d_8	100	13,107	6.00	No
ATRP-tBA-3	D_2O	66.7	16,384	3.00[c]	No
CVRP-AA-1	Dioxane-d_8	100	47,512	25.0	No
Linear	D_2O	100	n.r.[d]	n.r.[d]	No

[a] NaOD is 1 mol equivalent to acrylic acid (AA) units; [b] DCl (deuterium chloride) is ½ mol equivalent to AA units; [c] Degree of branching *DB* was not quantified and it was not checked whether the spectrum was quantitative; [d] Spectrum was not recorded

Quantitative NMR spectra

^{13}C NMR spectra were recorded for NMP-AA-4, and MADIX-AA-1-3 in this work and their *DB* quantified when possible.

DEPT-135 spectra were recorded to confirm signal assignment in some cases. In DEPT-135 spectra, CH- and CH_3 signals are positive and CH_2 signals are negative. The quaternary carbons exhibit no signal which helps confirm the assignment of the C_q branching signal.

^{1}H-^{1}H COSY and ^{1}H-^{13}C HMQC spectra were also recorded for MADIX-AA-1 and -2 in order to confirm some signal assignments. Since both spectra use ^{1}H NMR in at least one dimension, the ^{1}H NMR for both these PAAs were also included.

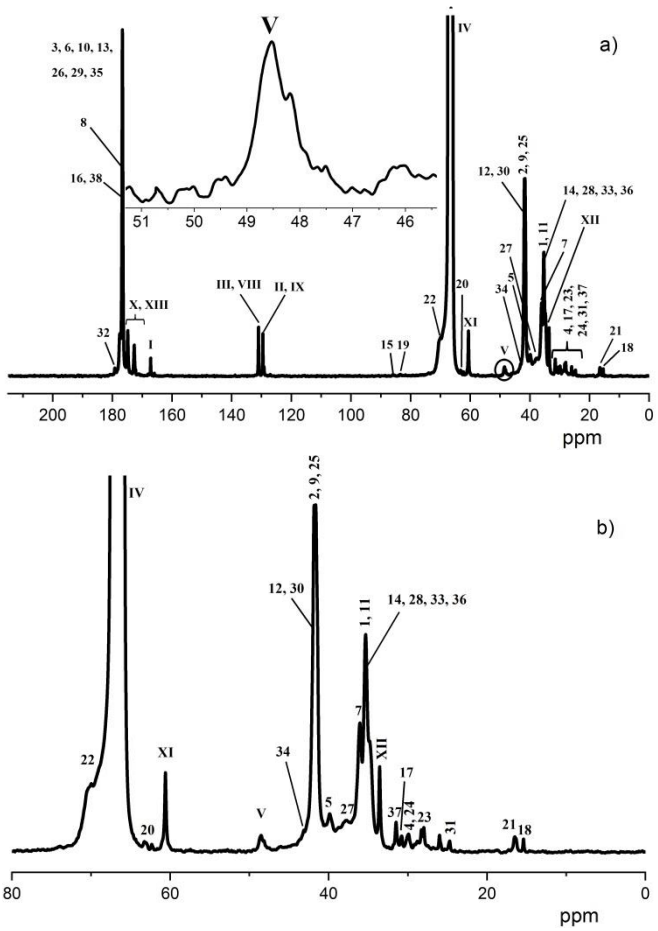

Figure S1. Solution-state quantitative ^{13}C NMR spectrum of NMP-AA-4 (75 MHz, D_2O): a) full spectrum with inset showing the region of the C_q signal of the branching point, b) 0 to 60 ppm region. See Figure S11, S12, 13b, S14a and S14c for chemical structures and Table S3 for signal assignment.

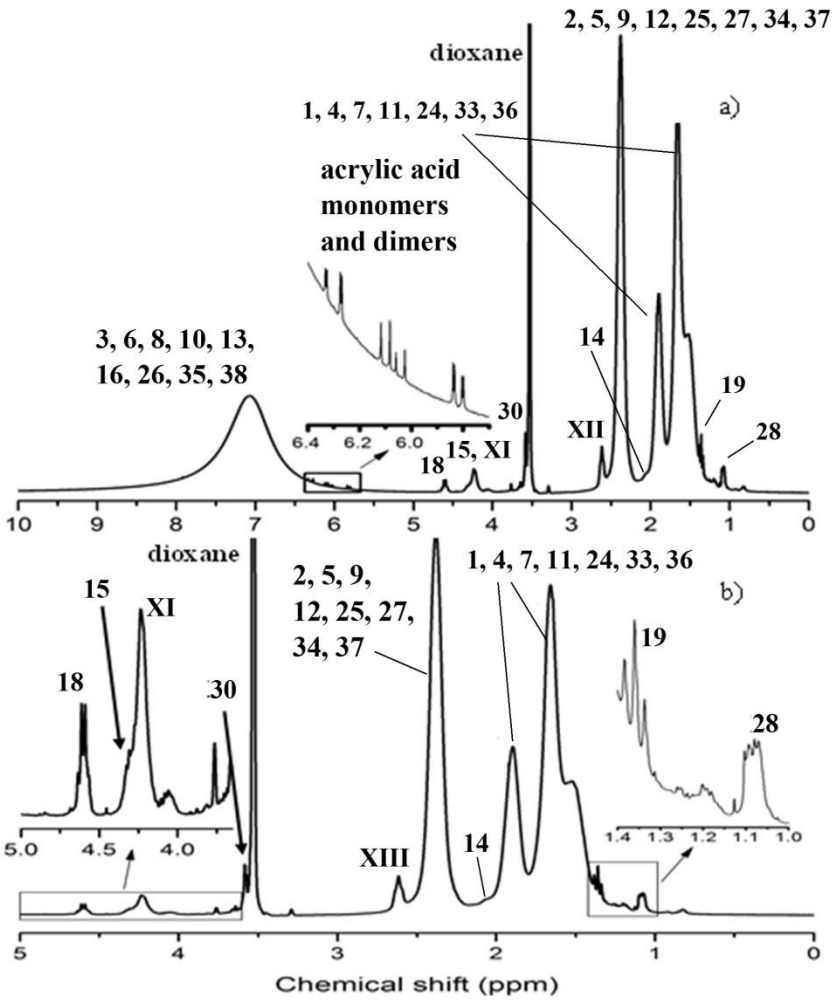

Figure S2. Solution-state ^{1}H NMR spectrum of MADIX-AA-1 (75.48 MHz, 1,4-dioxane-d_8): a) full spectrum with inset showing the vinylic signals from the residual monomers, b) region of the spectrum containing most signals of interest. See Figure S11, S12, S13a, S14b and S14c for chemical structures and Table S4 for signal assignment.

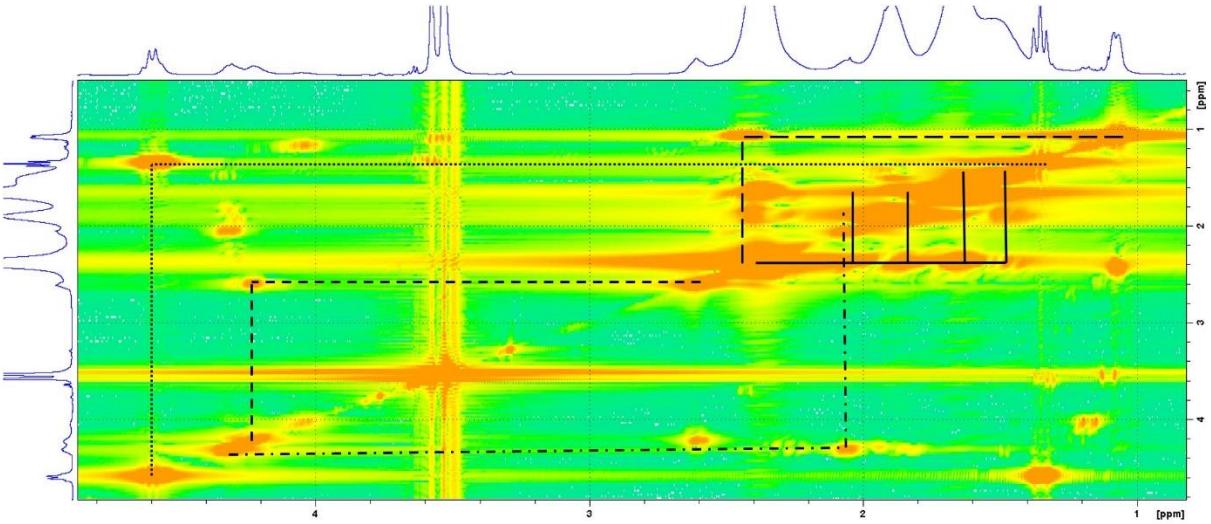

Figure S3. ^{1}H-^{1}H COSY spectrum of MADIX-AA-1 (75.48 MHz, 1,4-dioxane-d_8). 1D spectra are shown as projections. Observed correlations were between signals 18-19 (dotted lines), XI-XII (dashed lines), 27-28 (long dashed-lines), 14-15 (dotted-dashed lines) and backbone signals (full lines). See Figure S11, S12a, S13b and S13c for the chemical structure and Table S4 for signal assignment.

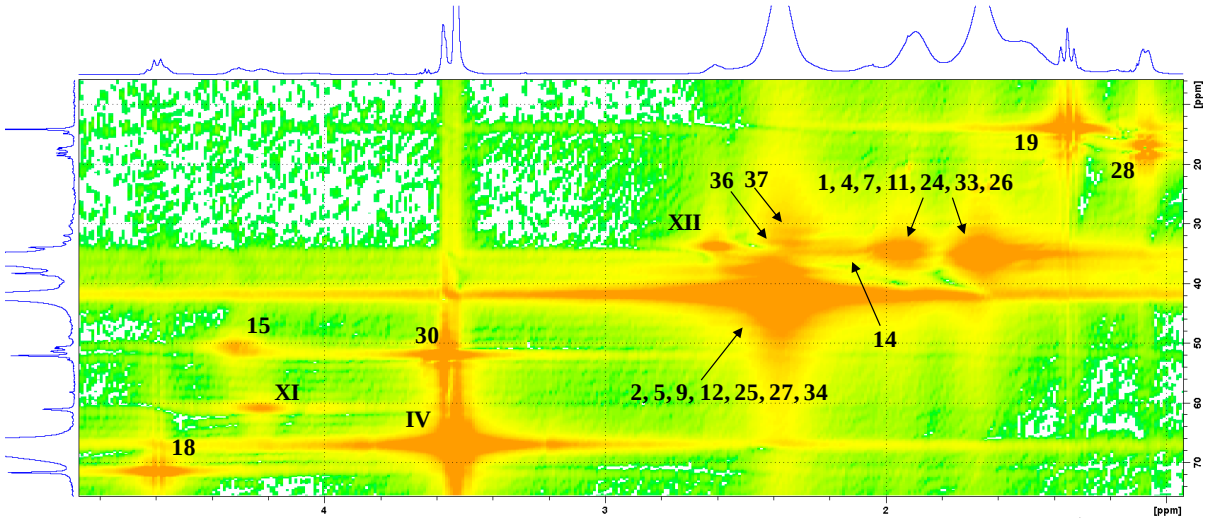

Figure S4. ^{1}H-^{13}C HMQC spectrum of MADIX-AA-2 in dioxane-d_8. Numbers represent the group assigned to cross peaks of interest (see Figure S14). 1D spectra are shown as projections. See Figure S11, S12, S13a, S14b and S14c for the chemical structure and Table S5 and S4 for signal assignment.

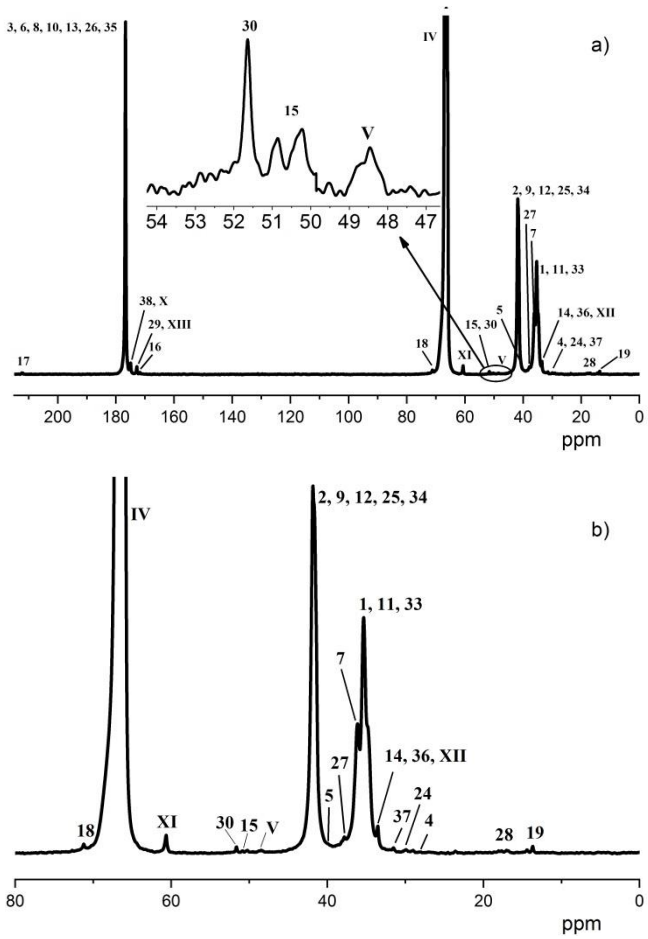

Figure S5. Solution-state quantitative ^{13}C NMR spectrum of MADIX-AA-1 (75.48 MHz, 1,4-dioxane-d_8): a) full spectrum with inset showing the region of the C_q signal of the branching point, b) 0 to 80 ppm region. See Figure S11, S12a, S13b and S13c for chemical structures and Table S5 for the signal assignment.

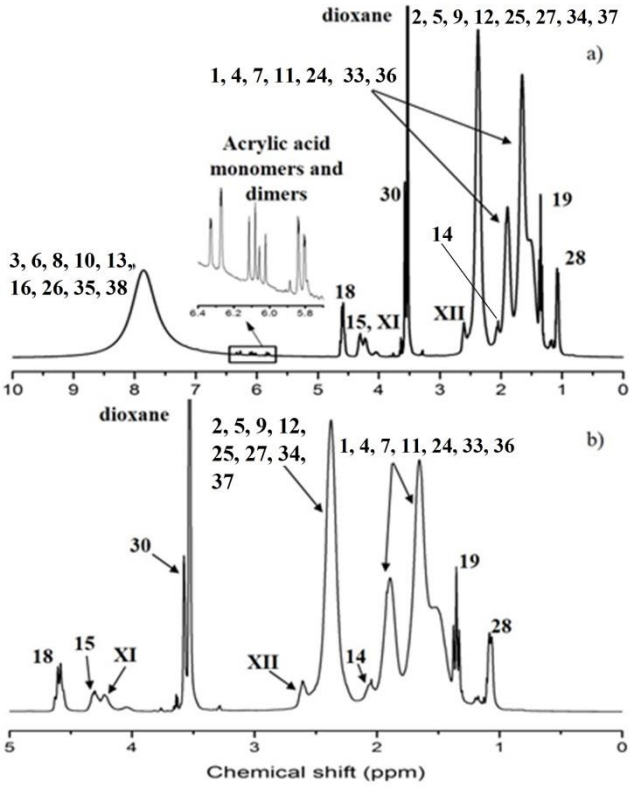

Figure S6. Solution-state ^{1}H NMR spectrum of MADIX-AA-2 (75.48 MHz, 1,4-dioxane-d_8): a) full spectrum with inset showing the vinylic signals from the residual monomers/AA dimer, b) region of the spectrum containing most signals of interest. See Figure S11, S12, S13a, S14b and S14c for chemical structures and Table S4 for signal assignment.

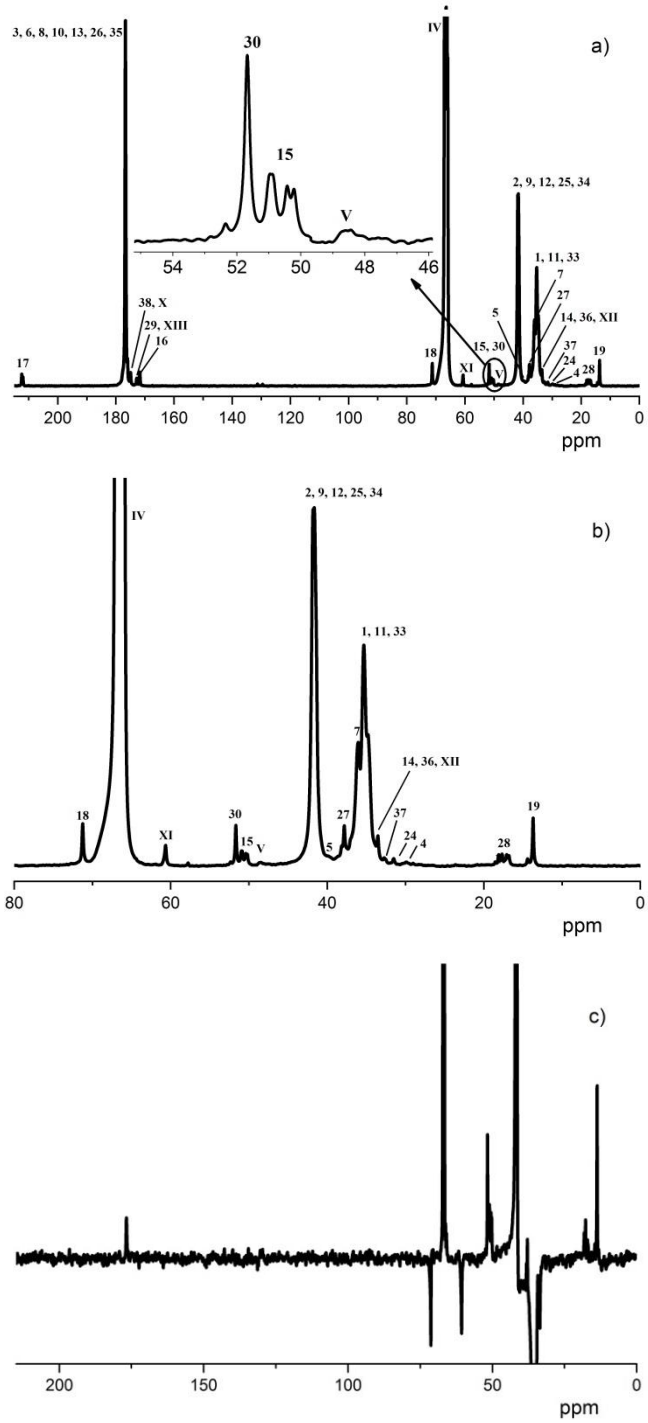

Figure S7. Solution-state ^{13}C NMR spectra of MADIX-AA-2 (75.48 MHz, 1,4-dioxane-d_8): a) full quantitative spectrum with inset showing the region of the C_q signal of the branching point, b) 0 to 80 ppm region of quantitative ^{13}C NMR spectrum and c) DEPT-135 spectrum. See Figure S11, S12, S13a, S14b and S14c for chemical structures and Table S4 for the signal assignment.

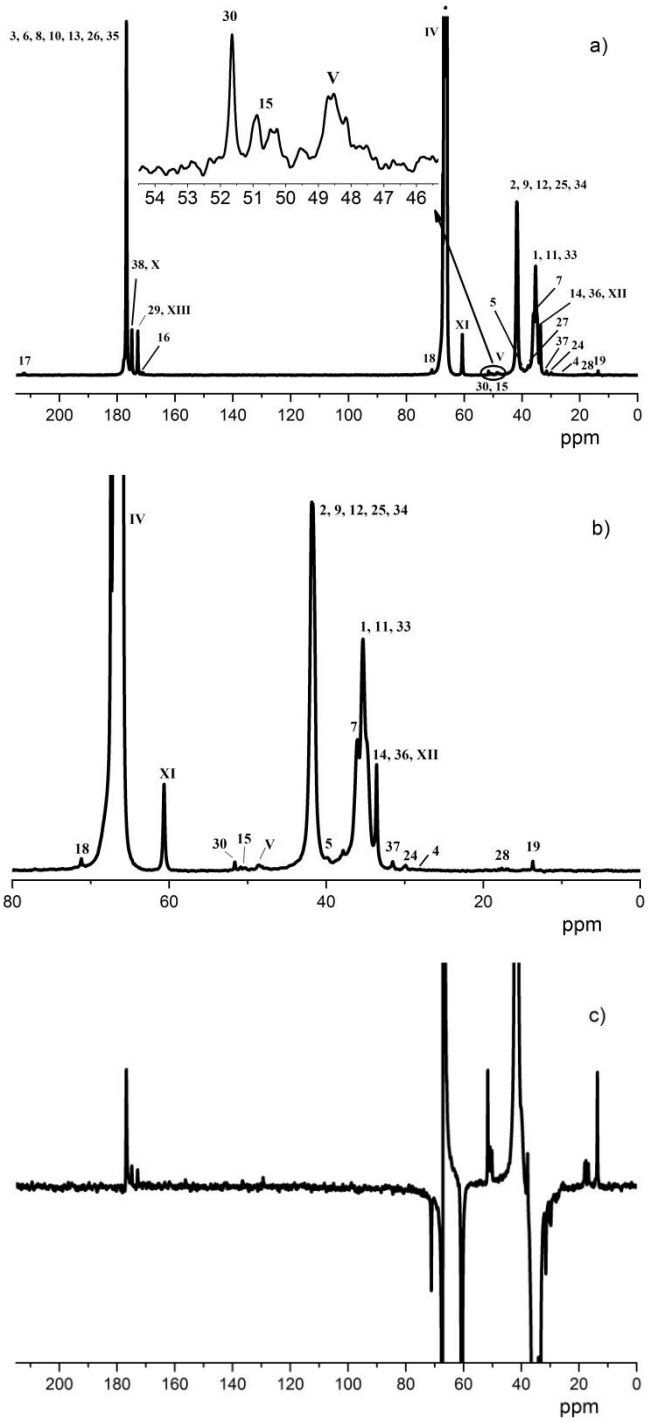

Figure S8. Solution-state ^{13}C NMR spectra of MADIX-AA-3 (75.48 MHz, 1,4-dioxane-d_8): a) full quantitative spectrum with inset showing the region of the C_q signal of the branching point, b) 0 to 80 ppm region of quantitative ^{13}C NMR spectrum and c) DEPT-135 spectrum. See Figure S11, S12, S13a, S14b and S14c for chemical structures and Table S5 for the signal assignment.

Non-quantitative NMR spectra

Preliminary ^{13}C NMR experiments of NMP-tBA-1 and ATRP-tBA-3 showed several limitations.

Difficulties in assigning the C_q signal of NMP-tBA-1 in D_2O (Figure S9a) was encountered as the presence of sodium deuteroxide (NaOD) may have resulted in the shift of several signals. Consequently, the C_q branching may have shifted into the backbone signal and thus completely overlap with it. It is also possible that the C_q signal was below the detection limit; however, an experimental time significantly longer than the initial 4 ½ days may be impractical. To amend the shift in the signals of NMP-tBA-1, deuterium chloride (DCl) was added (Figure S9b). No significance difference was observed between the chemical shifts of NMP-tBA-1 with and without DCl. Additionally, NMP-tBA-1 was also suspended in DMSO. No C_q signal was observed, possibly due to incomplete sample dissolution.

A high turbidity was observed for ATRP-tBA-3 in D_2O suggesting an incomplete dissolution. Incomplete solubility affects the accuracy of *DB*[1], thus the C_q signal observed in the ^{13}C NMR spectrum of ATRP-tBA-3 was not representative of the branching actually present in the sample. NaOD was added to increase the sample's solubility, but it caused a shift in signals. As a result the assignment of the C_q signal could not be confirmed.

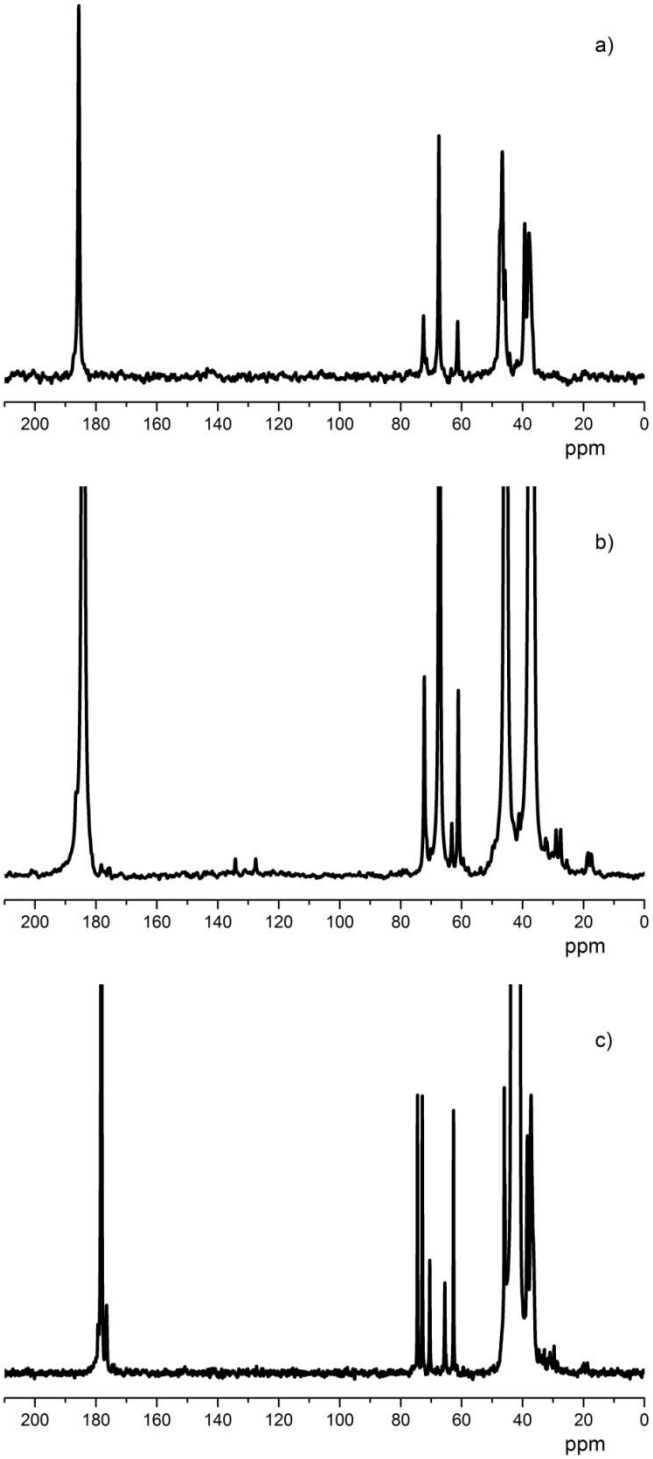

Figure S9. Solution-state ^{13}C NMR spectra of NMP-tBA-1 (75.48 MHz) in a) D_2O with NaOD, b) D_2O with NaOD and DCl and c) DMSO-d_6.

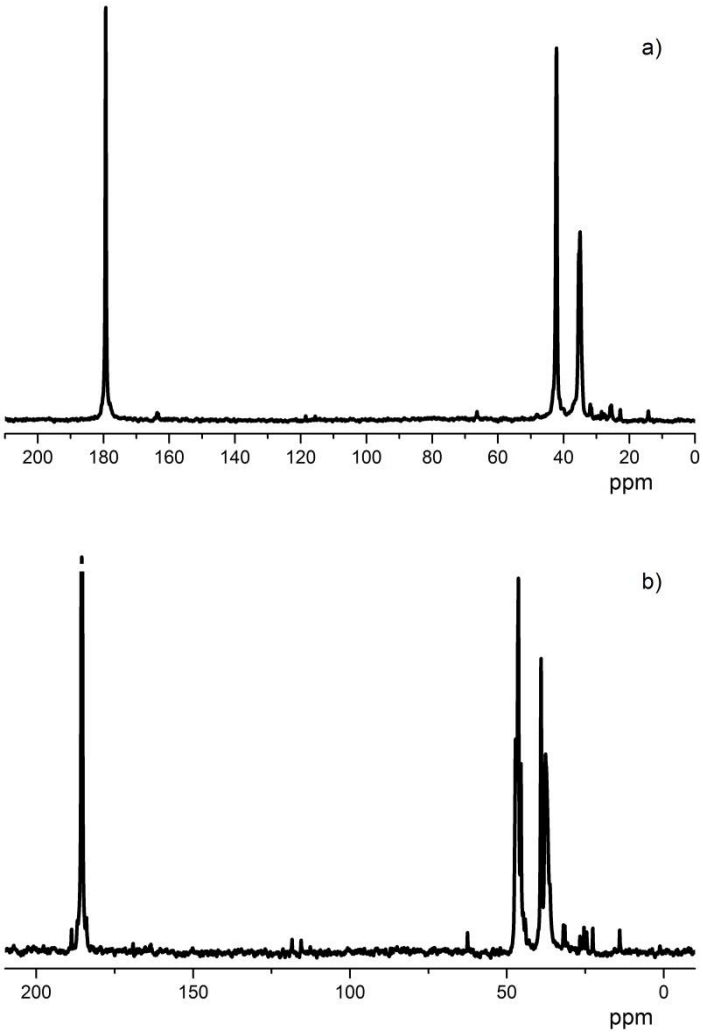

Figure S10. Solution-state ^{13}C NMR spectra of ATRP-tBA-3 (100 MHz) in a) D_2O and b) D_2O with NaOD.

Signal assignment

Full structure elucidation is shown in Table S3- S5 for the PAAs/PNaAs for which *DB* was quantified via ^{13}C NMR spectroscopy. Chemical shift estimation (Table S3-S5) was with ChemNMR (Cambridgesoft). For MADIX-AA-1 and 2, ^{1}H NMR and two-dimensional NMR spectra were also recorded for a comprehensive structure elucidation. For *DB* quantification the signals of interest are from C_q and the backbone. Overlapping signals of some end group with the polymer backbone ones are also accounted for in the M_n and *DB* quantification as shown in Equation S1-S26. In the case of overlapping signals, when DEPT-135 could not discriminate between the different possible assignments because the carbon atoms bear the same number of hydrogens, the signals were tentatively assigned. Presence of synthesis residues like acrylic acid and acrylic acid dimer was assumed unless confirmed otherwise via ^{1}H NMR spectroscopy. Chemical structures of PAA/PNaA as well as of the initiating and end groups with their group numbers have been assigned in an earlier publication (Figure S11 - S14 of [1]).

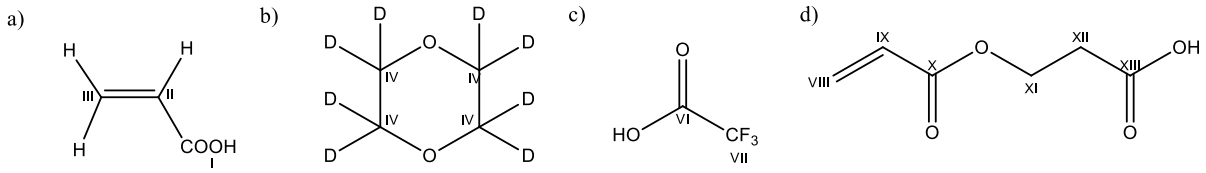

Figure S11. Chemical structure of a) AA, b) 1,4-dioxane-d_8, c) TFA and d) AA dimer. The labelled group numbers (GNs) are used for chemical shift assignment as published in [1].

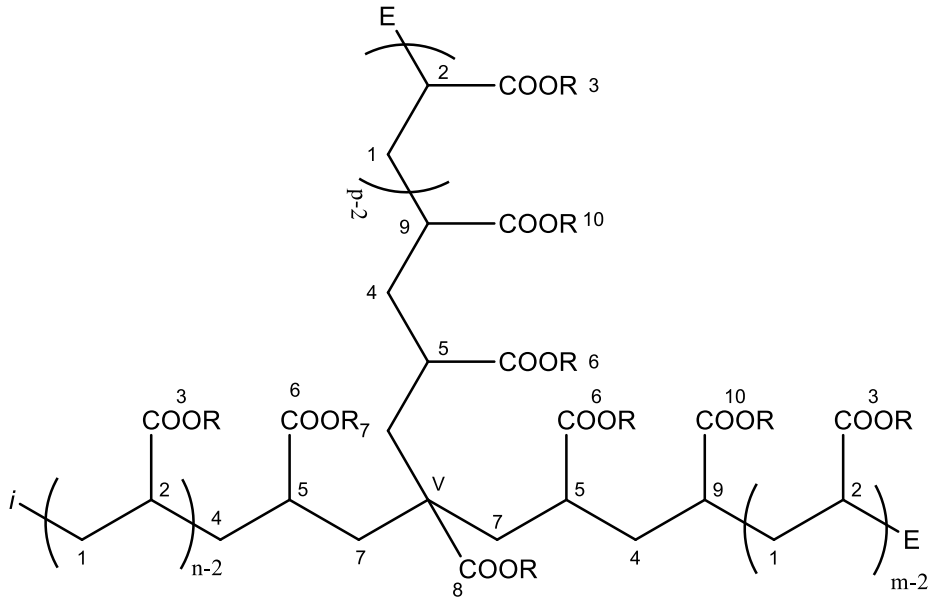

Figure S12. Chemical structure of PAAs/PNaA where R = H or R = Na. *i* represents the initiating group (see Figure S13) and E represents the chain-end (see Figure S14). The labelled GNs are used for chemical shift assignment as published in [1].

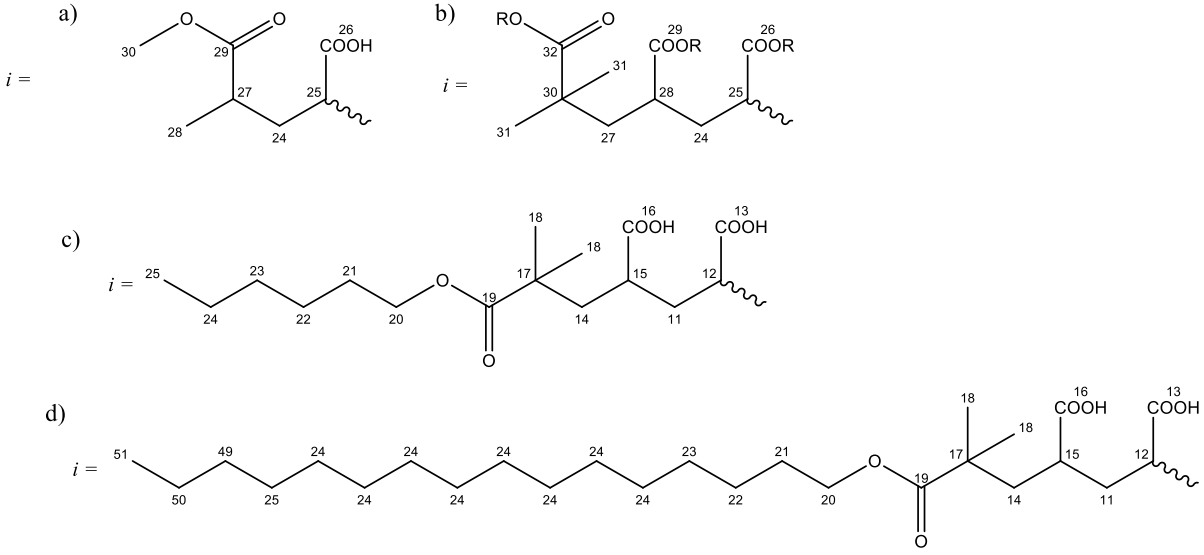

Figure S13. Chemical structure of the initiating groups (*i*) of a) MONAMS-initiated NMP PAA and MADIX PAA, b) BB-initiated NMP PAA/PNaA (where R = H or Na, which will be indicated accordingly in their signal assignment table), c) hexyl 2-bromoisobutyrate-initiated ATRP PAA, and d) hexadecyl-2-bromoisobutyrate-initiated ATRP PAA. The labelled GNs are used for chemical shift assignment as published in [1].

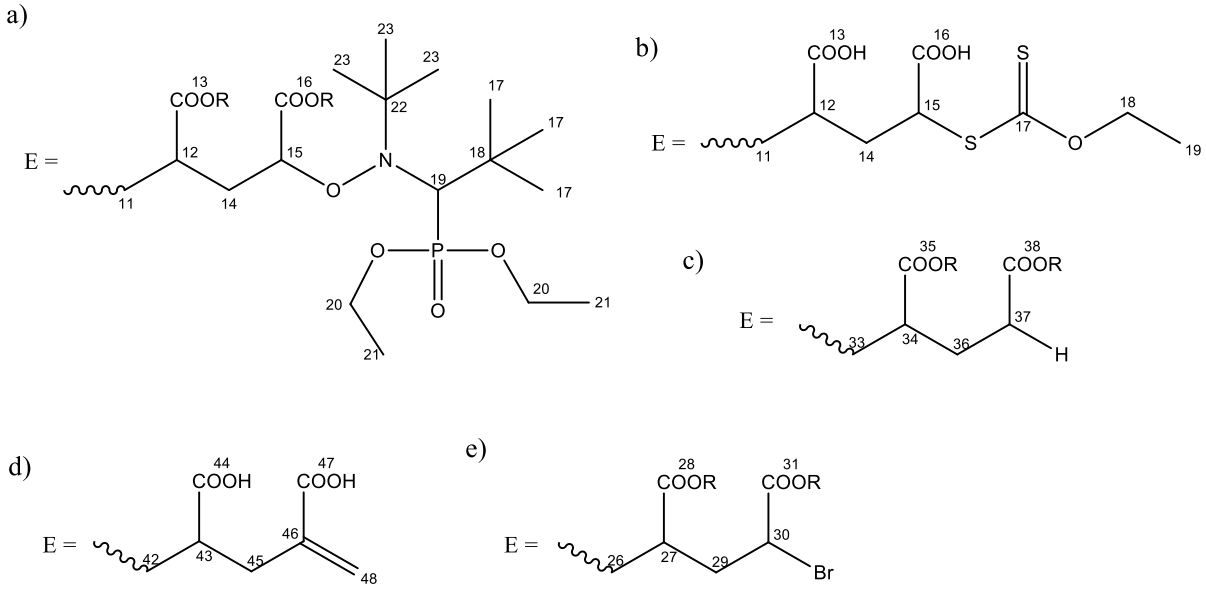

Figure S14. Chemical structure of different chain-ends (E) including the a) SG1 group, b) MADIX-agent end group, c) hydrogen, d) double-bond, e) bromine with labelled GNs that are used for chemical shift assignment as published in [1].

Table S3. Signal assignment for ^{13}C NMR spectrum of NMP-AA-4 in dioxane-d_8 (see Figure S1 for ^{13}C NMR spectra, see Figure S11, S12, S13b, S14a and S14c for definition of GNs, where R = H). OL stands for overlapping.

GN	***Estimated δ (ppm)***	***Observed δ (ppm), NMP-AA-4***
1, 11	26.2	32.1 – 39.2
2, 9, 25	41.3	39.2 – 46.8
3, 6, 10, 13, 26, 29, 35	182.9	169.6 – 181.6
4, 24	26.5	30.0 (OL with 1)
5	39.1	39.9 (OL with 2)
7	45.6	36.1 (OL with 1)
8	183.7	169.6 – 181.6 (OL with **3**)
12	37.3	39.2 – 46.8 (OL with **2**)
14?	29.4	33.6 (OL with **1**)
15	85.8	86.2 (OL with **19**)
16?, 38[a]?	173.2, 178.4[a], 177.3	169.6 – 181.6 (OL with **3**)
17	26.6	30.8
18	15.3	15.4
19	81.0	83.5 (OL with **15**)
20	62.2	63.3
21	16.3	16.5
22	70.4	70.0
23	26.1	28.0
27	50.0	37.8 (OL with **1**)
28	38.5	32.1 – 39.2 (OL with **1**)
30	41.6	39.2 – 46.8 (OL with **2**)
31	24.9	24.7
32	185.1	179.5
33	25.9	32.1 – 39.2 (OL with **1**)
34	43.5	43.1 (OL with **2**)
36?	29.6	33.6 (OL with 1)
37	27.4	31.5 (OL with **1**)
I	170.4	167.2
II, IX[a]	127.5	129.5
III, VIII[a]	134.1	131.0
IV	66.5	66.5
V	39.6	48.5
X, XIII	166.5, 177.3	172.0-175.6
XI	59.8	60.6
XII	33.8	33.6 (OL with **1**)

[a] Signals corresponding to two or more estimated δ values contain OL signals. Estimated δ values are listed in the same order as respective GNs. These signals cannot be confirmed with one-dimensional NMR only and are thus indicated by a question mark. This footnote applies to every table in this section.

Table S4. Signal assignments for ^{1}H NMR spectra of MADIX-AA-1 and -2 in dioxane-*d*$_8$ (see Figure S2 and S6 for ^{1}H NMR spectra, see Figure S11, S12, S13a, S14b and S14c for definition of GNs, where R=H).

GN	***Estimated δ (ppm)***	***Observed δ (ppm), MADIX-AA-1***	***Observed δ (ppm), MADIX-AA-2***
1	1.75	1.29 -2.16	1.23 – 2.16
2	2.35	2.16-2.87	2.16 – 2.87
3	11.0	5.50-8.50	6.50-9.00
4	1.75	1.29 -2.16 (OL with 1)	1.23 – 2.16 (OL with 1)
5	2.35	2.16-2.87 (OL with 2)	2.16 – 2.87 (OL with 2)
6	11.0	5.50-8.50	6.50-9.00
7	1.71	1.29 -2.16 (OL with 1)	1.23 – 2.16 (OL with 1)
8	11.0	5.50-8.50	6.50-9.00
9	2.35	2.16-2.87 (OL with 2)	2.16 – 2.87 (OL with 2)
10	11.0	5.50-8.50	6.50-9.00
11	1.75	1.29 -2.16 (OL with 1)	1.23 – 2.16 (OL with 1)
12	2.35	2.16-2.87 (OL with 2)	2.16 – 2.87 (OL with 2)
13	11.0	5.50-8.50	6.50-9.00
14	2.42	2.04-2.11 (OL with 1)	2.02-2.17 (OL with 1)
15	3.40	4.31 (OL with XI)	4.31 (OL with XI)
16	11.0	5.50-8.50	6.50-9.00
17	-	-	-
18	3.58	4.60	4.60
19	1.10	1.36 (OL with 1)	1.35 (OL with 1)
24	1.87	1.29 -2.16 (OL with 1)	1.23 – 2.16 (OL with 1)
25	2.35	2.16-2.87 (OL with 2)	2.16 – 2.87 (OL with 2)
26	11.0	5.50-8.50	6.50-9.00
27	2.49	2.16-2.87 (OL with 2)	2.16 – 2.87 (OL with 2)
28	1.19	1.08	1.08
29	-	-	-
30	3.68	3.58	3.58
33	1.75	1.29 -2.16 (OL with 1)	1.23 – 2.16 (OL with 1)
34	2.35	2.16-2.87 (OL with 2)	2.16 – 2.87 (OL with 2)
35	11.0	5.50-8.50	6.50-9.00
36	1.79	1.29 -2.16 (OL with 1)	1.23 – 2.16 (OL with 1)
37	2.33	2.16-2.87 (OL with 2)	2.16 – 2.87 (OL with 2)
38	11.0	5.50-8.50	6.50-9.00
II, III		5.80-6.34	5.80 – 6.34[a]
XI	4.42	4.24 (OL with 15)	4.23 (OL with 15)
X11	2.51	2.55-2.68 (OL with 2)	2.59-2.66 (OL with 2)

[a] The residual double bond signals were confirmed by comparing the splitting pattern observed for the residual double bond in reference [2].

Table S5. Signal assignment for ^{13}C NMR spectra of MADIX-AA-1 to -3 in 1,4-dioxane-*d*$_8$ (see Figure S5, S7 and S8 respectively for ^{13}C NMR spectra, see Figure S11, S12, S13a, S14b and S14c of for definition of GNs, where R=H).

GN	***Estimated δ (ppm)***	***Observed δ (ppm), MADIX-AA-1***	***Observed δ (ppm), MADIX-AA-2***	***Observed δ (ppm), MADIX-AA-3***
1	26.2	27.8 – 39.2	25.9 – 39.3	24.5 – 39.2
2, 9	41.3	39.2 – 46.7	39.3 – 47.3	39.2 – 46.1
3, 6, 10, 13, 26, 35	182.9	168.3 – 182.9	169.6 – 181.2	167.6 – 182.0
4	26.5	29.0 (OL with **1**)	29.0 (OL with **1**)	29.0 (OL with **1**)
5	39.1	39.9 (OL with **2**)	40.0 (OL with **2**)	39.9 (OL with **2**)
7	45.6	36.1 (OL with **1**)	36.1 (OL with **1**)	36.1 (OL with **1**)
8	183.7	168.3 – 182.9 (OL with **3**)	169.6 – 181.2 (OL with **3**)	167.6 – 182.0 (OL with **3**)
11, 33	25.9	27.8 – 39.2 (OL with **1**)	25.9 – 39.3 (OL with **1**)	24.5 – 39.2 (OL with **1**)
12	39.9	39.2 – 46.7 (OL with **2**)	39.3 – 47.3 (OL with **2**)	39.2 – 46.1 (OL with **2**)
14	30.8	33.5 (OL with **XII**)	33.5 (OL with **XII**)	33.6 (OL with **XII**)
15	47.0	49.8 – 51.7 (OL with 30)	39.3 – 47.3 (OL with **2**)50.2 - 51.6 (OL with 30)	51.2 -52.3 (OL with 30)
16	173.3	171.7 (OL with **3**)	171.8 (OL with **3**)	171.8 (OL with **3**)
17	215.3	212.2	212.2	212.4
18	70.0	71.2 (OL with **IV**)	71.2 (OL with **IV**)	71.2 (OL with **IV**)
19	14.0	13.7	13.7	13.7
24	27.0	29.9 (OL with **1**)	30.0 (OL with **1**)	29.9 (OL with **1**)
25	41.0	39.2 – 46.7 (OL with **2**)	39.3 – 47.3 (OL with **2**)	39.2 – 46.1 (OL with **2**)
27	35.9	37.8 (OL with **2**)	37.9 (OL with **2**)	37.9 (OL with **2**)
28	16.9	17.7	17.1	17.7
29	176.5	172.8 (OL with **X, XIII**)	172.9 (OL with **X, XIII**)	172.9 (OL with **X, XIII**)
30	52.2	51.7	51.6	51.7
34	43.5	39.2 – 46.7 (OL with **2**)	39.3 – 47.3 (OL with **2**)	39.2 – 46.1 (OL with **2**)
36	29.6	33.5 (OL with **XII**)	33.5 (OL with **XII**)	33.6 (OL with **XII**)
37	27.4	31.6 (OL with **1**)	31.5 (OL with **1**)	31.6 (OL with **1**)
38	178.4	175.0 (OL with **X, XIII**)	175.0 (OL with **X, XIII**)	174.9 (OL with **X, XIII**)
I	170.4	[c]	[c]	[c]
II, IX	127.5	[c]	130.0	[c]
III, VIII	134.1	[c]	131.6	[c]
IV	66.5	66.5	66.5	66.5
V	36.0	48.5	48.5	48.5
X, XIII	166.5, 177.3	172.7 – 175.7	172.7 - 175.6	172.7 - 175.6
XI	59.8	60.7	60.6	60.6
XII	33.8	33.5	33.5	33.6

For [a] see footnote a of Table S3.[b] Signal not assigned due to no corresponding signals in the estimated δ values. [c] Monomer/AA dimer are confirmed in ^{1}H NMR spectroscopy but are below the LOD in ^{13}C.

Fraction of dead chains

^{13}C NMR allows to detect the hydrogen end-groups in addition to the control agent end-groups and branching points. Hydrogen end-groups are assumed to originate mainly from either transfer to polymer or termination (by combination or disproportionation). The fraction of dead chains can thus be estimated as:

$$Dead\ chains\ (mol\%) = \frac{(H - C_q)\cdot 100}{H - C_q + L} \quad \text{(S1)}$$

where H is the signal integral of the -CH_2 end group, C_q is the signal integral of the quaternary carbon ("branching" signal, see Table S11) and L the signal integral of one carbon related to the control agent (living chain).

The results of the calculations of the dead chains are given in Table S6. Most of the ^{13}C NMR spectra exhibit a lower signal integral for the H-terminated region than for the quaternary carbon. This would numerically correspond to negative values for the fraction of dead chains. A value of 0 is simply indicated in the table in this case. The maximum possible fraction of dead chains has also been estimated based on the precision of each signal integral derived from the relevant *SNR*. The maximum fraction of dead chains is calculated from the highest possible value of H and the lowest value of Cq.

Table S6. Fraction of dead chains determined from ^{13}C NMR spectroscopy.

Sample	***Integration range of H signal (ppm)***	***Integration range of L signal (ppm)***	***Dead chains (mol%)***	***Maximum Dead chains (mol%)***
NMP-AA-1	31.13-31.25	24.84-52.57	0	0
NMP-AA-3	34.31-34.97	182.96-184.6	0	26
NMP-AA-4	31.18-31.67	25.49-23.79	0	0
NMP-AA-5 A	31.37-34.90		0	27
MADIX-AA-1	31.51-32.26	53.52-49.55	0	24
MADIX-AA-2	31.20-32.53	53.52-49.55	0.5	7
MADIX-AA-3	30.54-31.77	52.52-50.00	17	57
MADIX-AA-4 A		16.00-21.28	0	33
MADIX-AA-5 A	28.00-31.6	13.19-14.61	0	35
MADIX-AA-6	33.46-34.48	15.07-12.99	0 *	0 *
ATRP-tBA-1	30.8-32.66	12.56-15.52	0.2	13
ATRP-tBA-2	32.07-32.89	12.98-15.18	0	17

* the validity of the equation determining the fraction of dead chains is more questionable due to the possible occurrence of β-scission and polymerization of the formed macromonomers.

Theoretical M_n values

Most $M_{n(th)}$ values are from the literature (see main manuscript, Experimental, Polymerization). They are listed in Table S9.

In the case of MADIX-AA-3 to -6, a $M_{n(th)}$ of 10,000 g·mol^{-1} was targeted for each sample using the following equation:

$$M_{n(th)} = \frac{[AA]_0}{[AX]_0} \cdot x \cdot M_{AA} + M_{AX} \quad \text{(S2)}$$

where $[AA]_0$ and $[AX]_0$ are the initial concentrations (mol·L^{-1}) in acrylic acid monomer and xanthate (AX), respectively, x is the monomer conversion, M_{AA} and M_{AX} are the molar masses of AA and AX, respectively.

$M_{n(th)}$ values have then been more accurately calculated taking the formation of dead chains into account:

$$M_{n(th)} = \frac{[AA]_0}{[AX]_0 + \frac{2f}{2-k^{SS}}[I]_0 \left[1-\exp\left(-k_d \cdot t\right)\right]} \cdot x \cdot M_{AA} + M_{AX} \quad \text{(S3)}$$

where f is the efficiency of the initiator I, k^{ss} is the fraction of termination taking place by disproportionation, $[I]_0$ is the initial initiator concentration (mol·L^{-1}), k_d is the kinetic coefficient for the decomposition of the initiator, t is the polymerization time. $[AA]_0$, $[AX]_0$, x, $[I]_0$, and t are given in Table S1. Kinetic coefficients are listed in Table S7 and discussed below.

Table S7. Kinetic coefficients used to calculate $M_{n(th)}$ for samples synthesized by MADIX in dioxane at various temperatures T_{polym}. ACD stands for for 2,2'-azobis(4-methoxy-2.4-dimethyl valeronitrile), AIBN for 2,2'-azobisisobutyronitrile, ACBN for 1,1'-azobis(cyclohexanecarbonitrile),

Sample	T_{polym} (°C)	Initiator	Half-life (h)[a]	f	k^{SS}	*Dead chains*$_{th}$ (mol%)
MADIX-AA-3	35	ACD	5	0.1 to 0.8	0 to 0.1	0.9 to 6.9
MADIX-AA-4	60	AIBN (V50)	17	0.8[3]	0 to 0.1	0.5 to 3.7
MADIX-AA-5	90	ACBN	10	0.1 to 0.8	0 to 0.1	0.6 to 5.2
MADIX-AA-6	110	tert-Butyl peroxide	38	0.1 to 0.8	0 to 0.1	0.2 to 2.0

[a] from the 'Azo Polymerization Initiators Comprehensive Catalog', Wako.

In terms of initiator efficiency f, Minari et al.[4] consider f values between 0.2 and 0.5 for acrylic acid but for potassium persulfate as initiator. Torii et al. [5] determined efficiencies between 0.08 and 0.46 for initiation of acrylamide by non-ionic azo compounds in water. Wittenberg et al.[3] applied one of these values, 0.38, for the initiation of acrylic acid polymerization by VA-086. No efficiency by thermal initiator of acrylic acid in dioxane has been published as far as we could see. We thus hypothesized that the efficiency of the thermal

initiators used for this work was between 0.1 and 0.8 (0.8 being the value for AIBN as used for acrylic acid by [3]).

In terms of the fraction of termination by disproportionation in acrylic acid radical polymerization, k^{SS}, the initial literature assumed a similar contribution to termination of disproportionation and combination (k^{SS} = 0.5) [4]. Minari et al.[4] however did not observe the terminal double bonds (macromonomers) resulting from disproportionation and thus rather concluded that termination is mainly by combination (k^{SS} taken as 0). Our own NMR analysis on our samples show that macromonomers can be detected (see Figure S20) but they are detected only when the polymerization is performed at 120 °C in dioxane. This confirms that disproportionation is not the main termination mechanism and that the observed macromonomers are likely arising from some β-scission. Finally, Wittenberg et al.[3] best fit their data assuming k^{SS} is 0.05. k^{SS} was thus assumed to be most likely between 0 and 0.1 for the polymerizations of MADIX-AA-3 to -6 performed at different temperatures.

The calculation of the theoretical M_n with Equation S2 includes a calculation of the theoretical fraction of dead chains with the term:

$$Dead\ chains_{th}\ (mol\%) = \frac{\frac{2f}{2-k^{SS}}[I]_0\left[1-\exp\left(-k_d \cdot t\right)\right]}{[AX]_0 + \frac{2f}{2-k^{SS}}[I]_0\left[1-\exp\left(-k_d \cdot t\right)\right]} \quad \text{(S4)}$$

The theoretical fraction of dead chains calculated from Equation S4 is listed in Table S6. The range of values is consistent with the estimates of fractions of dead chains by ^{13}C NMR (Table S6).

M_n quantification from NMR

M_n was quantified using ^{13}C NMR in this work. Two ways to quantify M_n have been defined in the main manuscript (Equation 1 and 2). Like for *DB* quantification, signals overlapping with backbone signal should be taken into account. GN assignments of all the backbone signals were simplified to be GN1 for CH_2, GN2 for CH and GN3 for C=O unless specified otherwise. Particularly, GN15 was not integrated in the backbone signals as the chemical shift was too different. The equations for M_n quantification in PAAs/PNaAs for which overlapping signals with the backbone were observed are listed below, where M_m represents the molar mass of the monomer unit (which could be acrylic acid, sodium acrylate or *tert*-butyl acrylate). Table S8 indicates which equations are used for each sample.

$$M_n = \frac{I(\mathrm{C_{q,GNV}+CH_{2,GN1}+CH_{GN2}-CH_{GN15}+CH_{3,GN17,GN23}+CH_{2,GNXII}}) - 5I(\mathrm{CH_{3,GN30}}) - I(\mathrm{CH_{2,GNXI}})}{2 \times I(\mathrm{CH_{3,GN30}})} \times M_m \quad \text{(S5)}$$

$$M_n = \frac{I(\mathrm{C{=}O_{GN3}+C{=}O_{GN29}+C{=}O_{GNXIII}}) - I(\mathrm{CH_{3,GN30}}) - I(\mathrm{CH_{2,GNXI}})}{I(\mathrm{CH_{3,GN30}})} \times M_m \quad \text{(S6)}$$

$$M_n = \frac{I(\mathrm{C_{q,GNV}+CH_{2,GN1}+CH_{GN2}-CH_{GN15}+CH_{3,GN17,GN23,GN31}+CH_{2,GNXII}+C_{q,GN30}}) - 8I(\mathrm{CH_{3,GN18}}) - I(\mathrm{CH_{2,GNXI}})}{2 \times I(\mathrm{CH_{3,GN18}})} \times M_m \quad \text{(S7)}$$

$$M_n = \frac{I(\mathrm{C{=}O_{GN3}+C{=}O_{GN32}+C{=}O_{GNI,GNX,GNXIII}}) - I(\mathrm{CH_{3,GN18}}) - I(\mathrm{CH_{2,GNXI}}) - \frac{I(\mathrm{CH_{2,GNIII,GNVIII}}+\mathrm{CH_{2,GNII,GNIX}})}{2}}{I(\mathrm{CH_{3,GN18}})} \times M_m \quad \text{(S8)}$$

$$M_n = \frac{I(\mathrm{C_{q,GNV}+CH_{2,GN1}+CH_{GN2}-CH_{GN15}+C_{GN30}+CH_{2,GNXII}}) - I(\mathrm{CH_{2,GNXI}})}{2 \times I(\mathrm{C_{GN18}})} \times M_m \quad \text{(S9)}$$

$$M_n = \frac{I(\mathrm{C{=}O_{GN3}+C{=}O_{GN32}+C{=}O_{GNXIII}}) - I(\mathrm{C_{GN18}}) - I(\mathrm{CH_{2,GNXI}})}{I(\mathrm{C_{GN18}})} \times M_m \quad \text{(S10)}$$

$$M_n = \frac{I(\mathrm{CH_{2,GN1}}) + I(\mathrm{CH_{GN2}})}{2 \times I(\mathrm{CH_{3,GN21}})} \times M_m \quad \text{(S11)}$$

$$M_n = \frac{I(\mathrm{C{=}O_{GN3}}) - I(\mathrm{C_{GN21}})}{I(\mathrm{CH_{3,GN21}})} \times M_m \quad \text{(S12)}$$

$$M_n = \frac{I(\mathrm{C_{q,GNV}+CH_{2,GN1}+CH_{GN2}+C_{GN27}}) - I(\mathrm{CH_{3,GN19}})}{2 \times I(\mathrm{CH_{3,GN19}})} \times M_m \quad \text{(S13)}$$

$$M_n = \frac{I(\mathrm{C{=}O_{GN3}+C{=}O_{GN29}}) - I(\mathrm{CH_{3,GN19}})}{I(\mathrm{CH_{3,GN19}})} \times M_m \quad \text{(S14)}$$

$$M_n = \frac{I(\mathrm{C_{q,GNV}+CH_{2,GN1}+CH_{GN2}+C_{GN27}}) - I(\mathrm{CH_{3,GN28}})}{2 \times I(\mathrm{CH_{3,GN28}})} \times M_m \quad \text{(S15)}$$

$$M_n = \frac{I(\mathrm{C{=}O_{GN3}+C{=}O_{GN29}}) - I(\mathrm{CH_{3,GN28}})}{I(\mathrm{CH_{3,GN28}})} \times M_m \quad \text{(S16)}$$

$$M_n = \frac{I(\mathrm{C_{q,GNV}+CH_{2,GN1}+CH_{GN2}+C_{GN27}+CH_{2,GNXII}}) - I(\mathrm{CH_{3,GN19}}) - I(\mathrm{CH_{2,GNXI}})}{2 \times I(\mathrm{CH_{3,GN19}})} \times M_m \quad \text{(S17)}$$

$$M_n = \frac{I(\mathrm{C{=}O_{GN3}+C{=}O_{GN29}+CH_{2,GNXIII}}) - I(\mathrm{CH_{3,GN19}}) - I(\mathrm{CH_{2,GNXI}})}{I(\mathrm{CH_{3,GN19}})} \times M_m \quad \text{(S18)}$$

$$M_n = \frac{I(\mathrm{C_{q,GNV}+CH_{2,GN1}+CH_{GN2}+CH_{2,GN17,GN21-24}+CH_{3,GN18}}) - 7I(\mathrm{CH_{3,GN25}})}{2 \times I(\mathrm{CH_{3,GN25}})} \times M_m \quad \text{(S19)}$$

$$M_n = \frac{I(\mathrm{C{=}O_{GN3}}+\mathrm{C{=}O_{GN19}})-I(\mathrm{CH_{3,GN25}})}{I(\mathrm{CH_{3,GN25}})} \times M_m \quad \text{(S20)}$$

$$M_n = \frac{I(\mathrm{C_{q,GNV}}+\mathrm{CH_{2,GN1}}+\mathrm{CH_{GN2}}+\mathrm{CH_{2,GN17-18,GN21-25,GN49-50}})-17I(\mathrm{CH_{3,GN51}})}{2 \times I(\mathrm{CH_{3,GN51}})} \times M_m \quad \text{(S21)}$$

$$M_n = \frac{I(\mathrm{C{=}O_{GN3}}+\mathrm{C{=}O_{GN19}})-I(\mathrm{CH_{3,GN51}})}{2 \times I(\mathrm{CH_{3,GN51}})} \times M_m \quad \text{(S22)}$$

$$M_n = \frac{I(\mathrm{C_{q,GNV}}+\mathrm{CH_{2,GN1}}+\mathrm{CH_{GN2}}+\mathrm{C_{GN17}}+\mathrm{CH_{3,GN18}}+\mathrm{CH_{2,GNXII}})-3(CN_{\mathrm{GN19}})-I(\mathrm{CH_{2,GNXI}})}{2 \times I(\mathrm{CN_{GN19}})} \times M_m \quad \text{(S23)}$$

$$M_n = \frac{I(\mathrm{C{=}O_{GN3}}+\mathrm{C{=}O_{GNXIII}})-I(\mathrm{CH_{2,GNXI}})}{I(\mathrm{CN_{GN19}})} \times M_m \quad \text{(S24)}$$

Table S8. Equations used for M_n quantification in PAAs and PNaAs

Sample	***Equations***
NMP-AA-1 and -3	S5[a], S6
NMP-AA-4	S7[a],S8[a]
NMP-AA-5	S9[a], S10[a]
NMP-AA-6	S11, S12
MADIX-AA-1-3, MADIX-AA-5	S13[a], S14[a, b]
MADIX-AA-4	S15, S16
MADIX-AA-6	S17[a], S18[a]
ATRP-tBA-1	S19, S20
ATRP-tBA-2	S21, S22
CVRP-AA-1	S23, S24

[a] Calculation was based on the assumption of 100 % livingness. [b] Equations S13 and S15, as well as Equations S14 and S16 can be used interchangeably for their respective samples; however, the assigned equation was preferred due to stronger signals present for that specific equation.

Table S9. $M_{n(th)}$ and $M_{n(ex)}$ of several PAAs/PNaAs. $M_{n(ex)}$ were obtained by several methods including SEC ($M_{n(SEC)}$), ^{1}H NMR spectroscopy ($M_{n(1H\ NMR)}$) and ^{13}C NMR spectroscopy ($M_{n(13C\ NMR)}$). As mentioned, $M_{n(13C\ NMR)}$ was calculated in 2 different ways as shown below. n.d. stands for not determined.

Sample	$M_{n(th)}$ ($g \cdot mol^{-1}$)	$M_{n(SEC)}$ ($g \cdot mol^{-1}$)	$M_{n(1H\ NMR)}$ ($g \cdot mol^{-1}$)	$M_{n(13C\ NMR,\ bb)}$ ($g \cdot mol^{-1}$)	$M_{n(13C\ NMR,\ COOH)}$ ($g \cdot mol^{-1}$)
NMP-AA-1	4,900	6,900	n.d.	6,810 ± 350	6,810 ± 350
NMP-AA-3	4,600	7,800	n.d.	6,700 ± 400	6,660 ± 400
NMP-AA-4	4,150	7,200	n.d.	12,270 ± 870	11,730 ± 830
NMP-AA-5	2,100	10,000	n.d.	5,910 ± 470	5,590 ± 440
NMP-AA-6	2,700	12,000	n.d.	5,980 ± 1,400	6,020 ± 1,410
MADIX-AA-1	10,000	21,000[a]; 20,300[b]	n.d.	5,600 ± 510	5,560 ± 520
MADIX-AA-2	2,000	2,200[a]; 12,400[b]	n.d.	1,760 ± 50	1,710 ± 50
MADIX-AA-3	9,000 to 9,600	7,500	n.d.	11,700 ± 750	12,270 ±790
MADIX-AA-4 A	9,300 to 9,600	21,900	n.d.	2,830 ± 110	2,960 ± 120
MADIX-AA-4 B	9,300 to 9,600	21,900	n.d.	2,480 ± 190	2,700 ± 210
MADIX-AA-5 A	9,100 to 9,600	20,000	n.d.	11,180 ± 1,360	11,540 ± 1,404
MADIX-AA-5 B	9,100 to 9,600	20,000	n.d.	10,690 ± 1,290	11,470 ± 1,350
MADIX-AA-6	8,900 to 9,000	17,000	n.d.	11,660 ± 1,390	11,720 ± 1,400
ATRP-tBA-1	6,810	2,880	4,220	11,310 ± 800	11,020 ± 780
ATRP-tBA-2	6,750	n.d.	9,390	6,660 ± 250	6,230 ± 230
CVRP-AA-1	n.d.	33,700	n.d.	32,300 ± 8,620	32,870 ± 8,770

[a] from universal calibration; [b] from MALLS detection

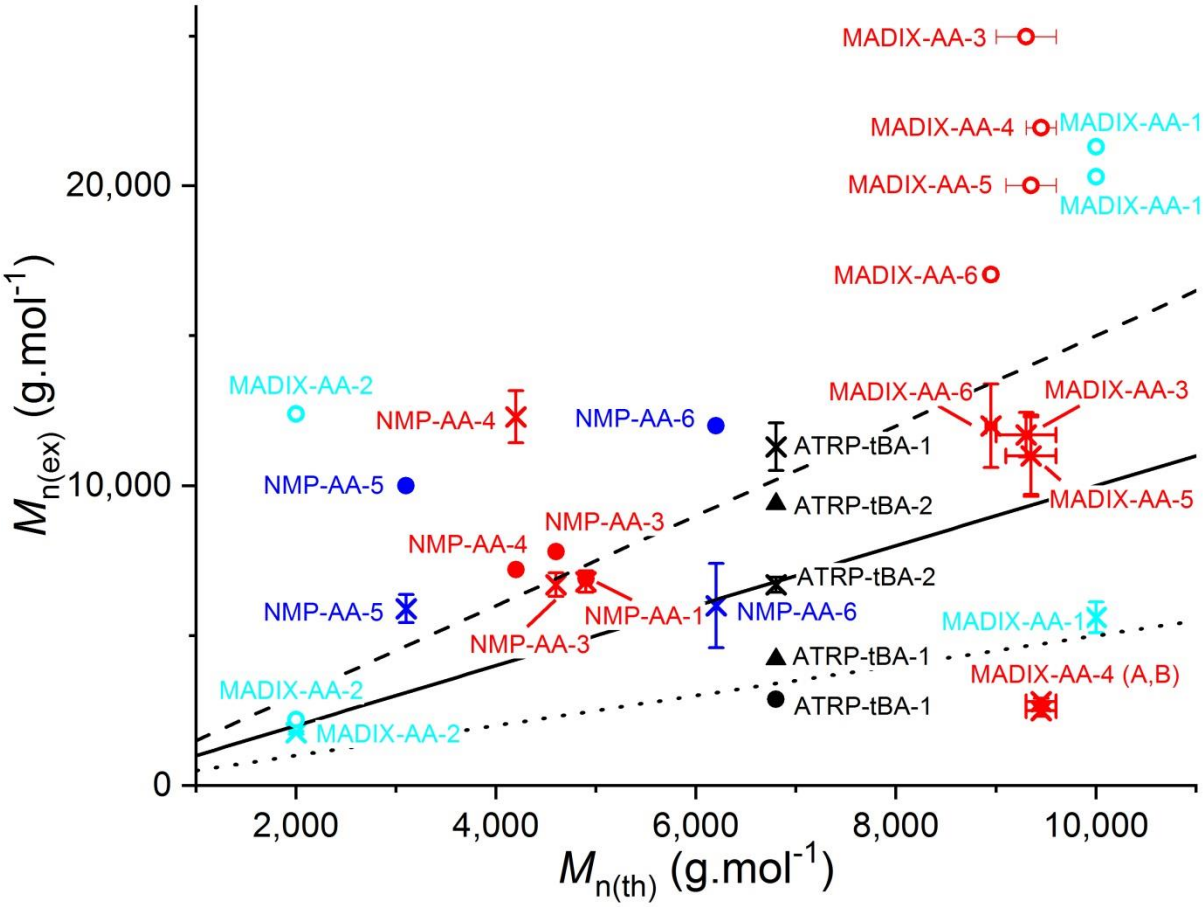

Figure S15. Larger version of Figure 1 with data points labelled with sample codes. The plotted data is also listed in Table S9. Comparison of $M_{n(th)}$ with $M_{n(ex)}$ determined for PAAs/PNaAs synthesized in dioxane using ^{13}C (✕) NMR spectroscopy or organic-phase (●) and aqueous-phase (○) SEC, for PAAs/PNaAs synthesized in bulk using ^{1}H (▲) and ^{13}C (✕) NMR spectroscopy or organic-phase SEC (●), for PAAs/PNaAs synthesized in toluene using ^{1}H (▲) and ^{13}C (✕) NMR spectroscopy, for PAAs/PNaAs synthesized in water/ethanol using ^{13}C NMR spectroscopy (✕) or aqueous-phase SEC (○), for PAAs/PNaAs synthesized in water using ^{13}C NMR spectroscopy (✕) or organic-phase SEC (●). The error bars are based on the precision estimated from the sensitivity of the NMR measurement (Y error bars) or the uncertainty on some kinetic parameters (X error bars). — is the diagonal ($M_{n(th)}$=$M_{n(ex)}$), – – represents when $M_{n(th)}$ was 50 % lower than $M_{n(ex)}$, and ····· represents when $M_{n(ex)}$ was 50 % lower than $M_{n(th)}$.

DB quantification

For this study, all PAA/PNaA displayed signals overlapping with the backbone signals which need to be accounted for. Two approaches allow to quantify *DB* as in [1] (Equation 1 and 2). Similar equations were derived for *DB* quantification in PAAs/PNaAs for which signals overlap with the backbone signals (Equation S25 and S26). The slightly different chemical shifts of the signals of the backbone in the polymer were simplified to be GN1 for CH_2, GN2 for CH and GN3 for C=O for all the corresponding signals of the backbone for the equation unless specified otherwise. GNs used in these equations will refer back to the signal assignments of their corresponding sample in this supporting information and in [1]. Note that sometimes the signal for GN15 is not integrated together with the other backbone signals as it is resolved from the backbone signals.

$$DB\ (\%) = \frac{I(\mathrm{C_{q,GNV}})\times 2\times 100}{I(C_{\mathrm{q,GNV}})+I(\mathrm{C_{q,GNV}+CH_{2,GN1}+CH}_{\mathrm{GN2}}-\mathrm{CH}_{\mathrm{GN15}}+\mathrm{CH_{3,GN17,GN23,GN31}+CH_{2,GNXII}+C_{q,GN30}})-9I(\mathrm{CH_{3,GN18}})-I(\mathrm{CH_{2,GNXI}})} \quad \text{(S25)}$$

$$DB\ (\%) = \frac{I(\mathrm{C_{q,GNV}})\times 100}{I(\mathrm{C{=}O_{GN3}+C{=}O_{GN32}+C{=}O_{GNI,GNVIII,GNX,GNXIII}})-I(\mathrm{CH_{3,GN18}})-2I(\mathrm{CH_{2,GNXI}})-\frac{I(\mathrm{CH_{2,GNIII,GNVIII}+CH_{2,GNII,GNIX}})-2I(\mathrm{CH_{2,GNIX}})}{2}}$$
$$= \frac{I(\mathrm{C_{q,GNV}})\times 100}{I(\mathrm{C{=}O_{GN3}+C{=}O_{GN32}+C{=}O_{GNI,GNVIII,GNX,GNXIII}})-I(\mathrm{CH_{3,GN18}})-I(\mathrm{CH_{2,GNXI}})-\frac{I(\mathrm{CH_{2,GNIII,GNVIII}+CH_{2,GNII,GNIX}})}{2}} \quad \text{(S26)}$$

Table S10. Equations used for *DB* quantification in PAAs and PNaAs

Sample	***Equations***
NMP-AA-1 and -3	S1[a] of [1], S2 of [1]
NMP-AA-4	S25[a], S26[a]
NMP-AA-5	S3[a] of [1], S4[a] of [1]
MADIX-AA-1-3 and -5	S7[a,b] of [1], S8[a,b] of [1]
MADIX-AA-4	S5[a,b] of [1],S6[a,b] of [1]
MADIX-AA-6	S9[a] of [1], S10[a] of [1]
ATRP-tBA-1	S11 of [1], S12 of [1]
ATRP-tBA-2	S13 of [1], S14 of [1]
CVRP-AA-1	S15 of [1], S16 of [1]

[a] Calculation was based on the assumption of 100 % livingness. [b] Equations S5 and S7, as well as Equations S6 and S8 can be used interchangeably for their respective samples; however, the assigned equation was preferred due to stronger signals present for that specific equation.

Table S11. Average *DB* of several PAAs/PNaAs quantified through the signals from the backbone (Equation 1 or one of its derivatives) or the carboxylic acid group (Equation 2 or one of its derivatives). NMP-AA-6 displayed a C_q signal below detection limit and thus its *DB* was not quantified.

Sample	***Integration range of C_q signal (ppm)***	***DB (%) backbone***	***DB (%) COOH***
NMP-AA-1	46.7 - 50.0	3.1 ± 0.2	3.1 ± 0.2
NMP-AA-3	46.5 - 50.9	3.3 ± 0.2	3.4 ± 0.2
NMP-AA-4	46.7 - 50.8	3.2 ± 0.2	3.4 ± 0.2
NMP-AA-5 A	49.5 – 53.2	2.0 ± 0.6	2.1 ± 0.7
NMP-AA-6		< 1.2 [b]	
MADIX-AA-1	47.6 - 49.5	0.3 ± 0.1	0.3 ± 0.1
MADIX-AA-2	46.5 - 49.5	0.7 ± 0.1	0.7 ± 0.1
MADIX-AA-3	46.1 – 49.9	1.2 ± 0.2	1.2 ± 0.2
MADIX-AA-4 A	46.5 – 49.6	2.4 ± 0.2	2.3 ± 0.1
MADIX-AA-4 B	46.7 – 49.9	2.1 ± 0.1	1.9 ± 0.1
MADIX-AA-5 A	47.0 – 49.5	2.3 ± 0.2	2.3 ± 0.2
MADIX-AA-5 B	47.0 – 49.5	2.5 ± 0.3	2.4 ± 0.2
MADIX-AA-6	47.0 – 49.7	3.3 ± 0.2	3.3 ± 0.2
ATRP-tBA-1[a]	46.5 - 50.1	1.6 ± 0.3	1.7 ± 0.3
ATRP-tBA-2[a]	46.4 - 49.3	1.1 ± 0.1	1.1 ± 0.2
CVRP-AA-1	46.3 - 50.0	2.6 ± 0.2	2.6 ± 0.2

[a] *DB* is an overestimated value because of a possible overlap between GNV and GN17 (GN17 not taken into account in the DB quantification). [b] The C_q signal had an SNR < 3, *DB* was overestimated via 1-point calibration (see next section).

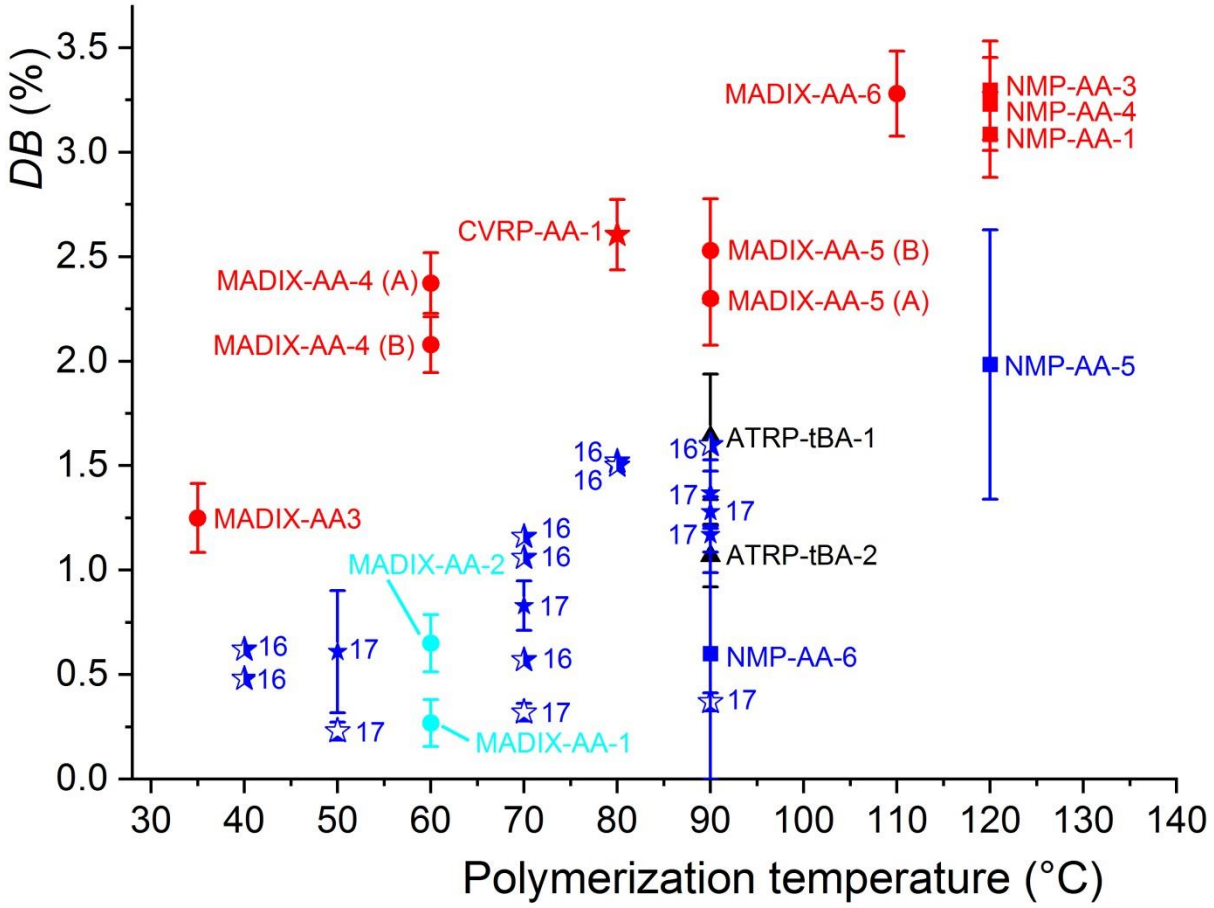

Figure S16. Larger version of Figure 2 with data points labelled with sample codes (for samples analysed in this work) or the relevant literature reference (16 or 17 of main manuscript, see below). The plotted data is also listed in Table S11 for samples analysed in this work. *DB* of PAAs/PNaAs synthesized in dioxane by NMP (■), MADIX (●) and CVRP (★), in bulk with ATRP (▲), in toluene with CVRP with CTA (☆), in water/ethanol with MADIX (●), and in water with NMP (■), CVRP (★ from 16, ★ from 17), and CVRP with CTA (☆from 17). The error bars are based on the precision estimated from the sensitivity of the NMR measurement. The vertical bar linking the red stars represents the large uncertainty on the monomer conversion for sample CVRP-AA-1.

Reference 16: N. F. G. Wittenberg, C. Preusser, H. Kattner, M. Stach, I. Lacík, R. A. Hutchinson and M. Buback, Macromol. React. Eng., 2015, 10, 95-107;

Reference 17: J.-B. Lena, A. K. Goroncy, J. J. Thevarajah, A. R. Maniego, G. T. Russell, P. Castignolles and M. Gaborieau, Polymer, 2017, 114, 209-220.

***DB* overestimation**

For NMP-AA-6 the C_q signal was below the detection limit (signal-to-noise ratio $SNR < 3$). It also overlapped with the backbone. Hence, the *DB* value was overestimated through the determination of the maximal possible *DB* value, DB_{max}. A one point calibration between the ratio of the *SNR*s of the backbone and C_q signals (SNR_{BB}/SNR_{Cq}) and the ratio of the integrals of the backbone and C_q signals (I_{BB}/I_{Cq}) was established using sample NMP-AA-3. This 1-point calibration was then used to estimate the maximal possible value of I_{Cq}/I_{BB} based on a maximal possible SNR_{Cq} value of 3 and on the experimental value of SNR_{BB} for NMP-AA-6. This was in turn used to determine DB_{max} as follows:

$$DB_{\max}\,(\%) = \frac{\left(\frac{I_{Cq}}{I_{BB}}\right)_{max} \times 200}{1+\left(\frac{I_{Cq}}{I_{BB}}\right)_{max}} \qquad \text{(S27)}$$

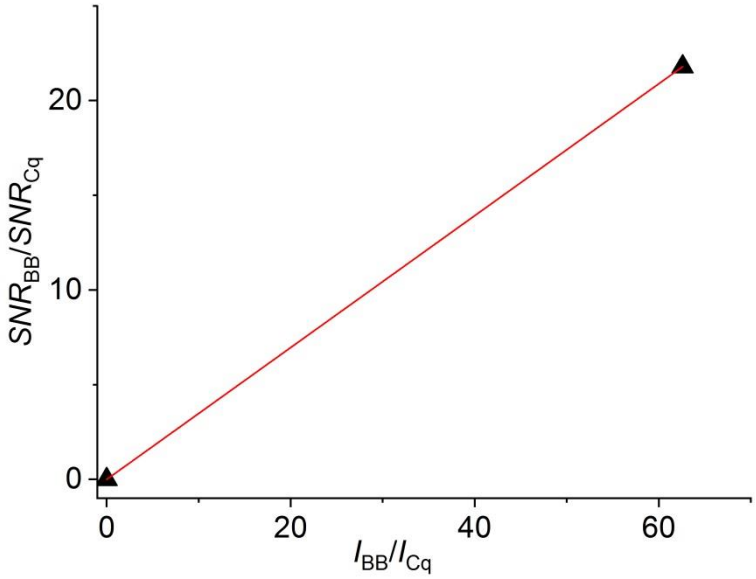

Figure S17. 1-point calibration of SNR_{BB}/SNR_{Cq} vs I_{BB}/I_{Cq} established with NMP-AA-3 . y = 0.34829 *x*

***DB* quantification for poly(*n*-butyl acrylates)[6]**

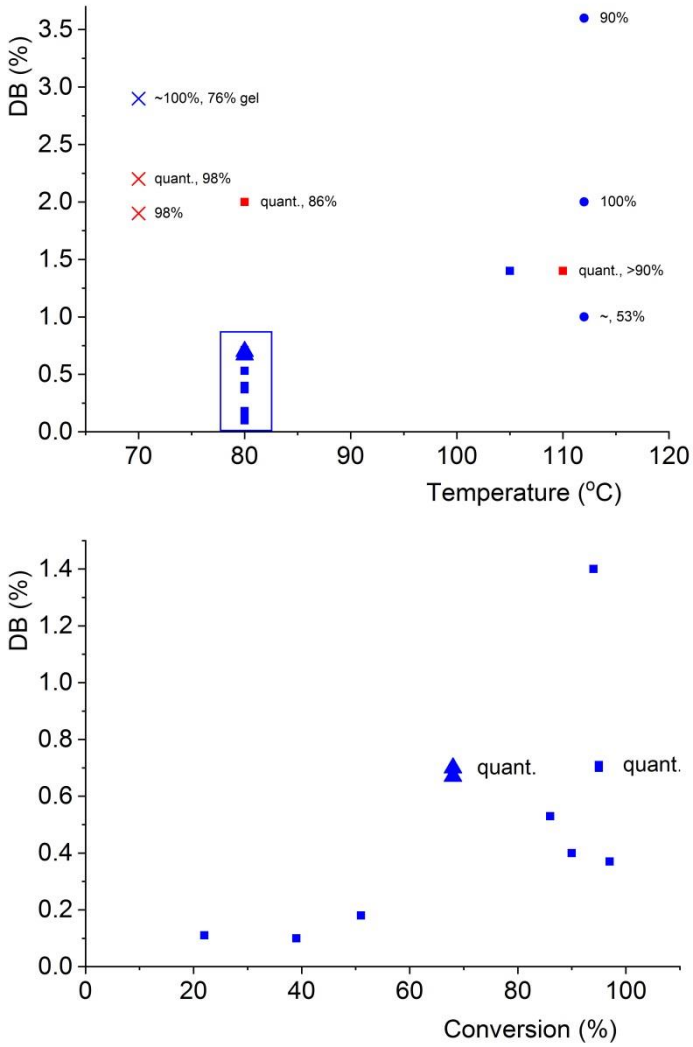

Figure S18. *DB*(%) of several poly(*n*-butyl acrylate)s reported in [6]. They were synthesized at different temperatures and with different polymerization techniques including CVRP (cross), ATRP (square), RAFT (triangle) and NMP (circle) either in bulk (blue) or in 50 % xylene (red). On the top graph *DB* is plotted versus temperature. The percentages shown next to the data points are conversion values. The label '76% gel' identifies a sample reported in [6] as containing 76% gel fraction. The region boxed in the top graph represents poly(*n*-butyl acrylate)s with similar *DB*(%) synthesized at the same temperature; the data from this region was also plotted as *DB*(%) versus conversion (bottom graph). *DB* values obtained from quantitative NMR spectra are identified through the label 'quant.' next to the corresponding data point. No error bar is shown since the uncertainty was not given in reference [6].

Relation between branching and the relative difference between $M_{n(ex)}$ and $M_{n(th)}$

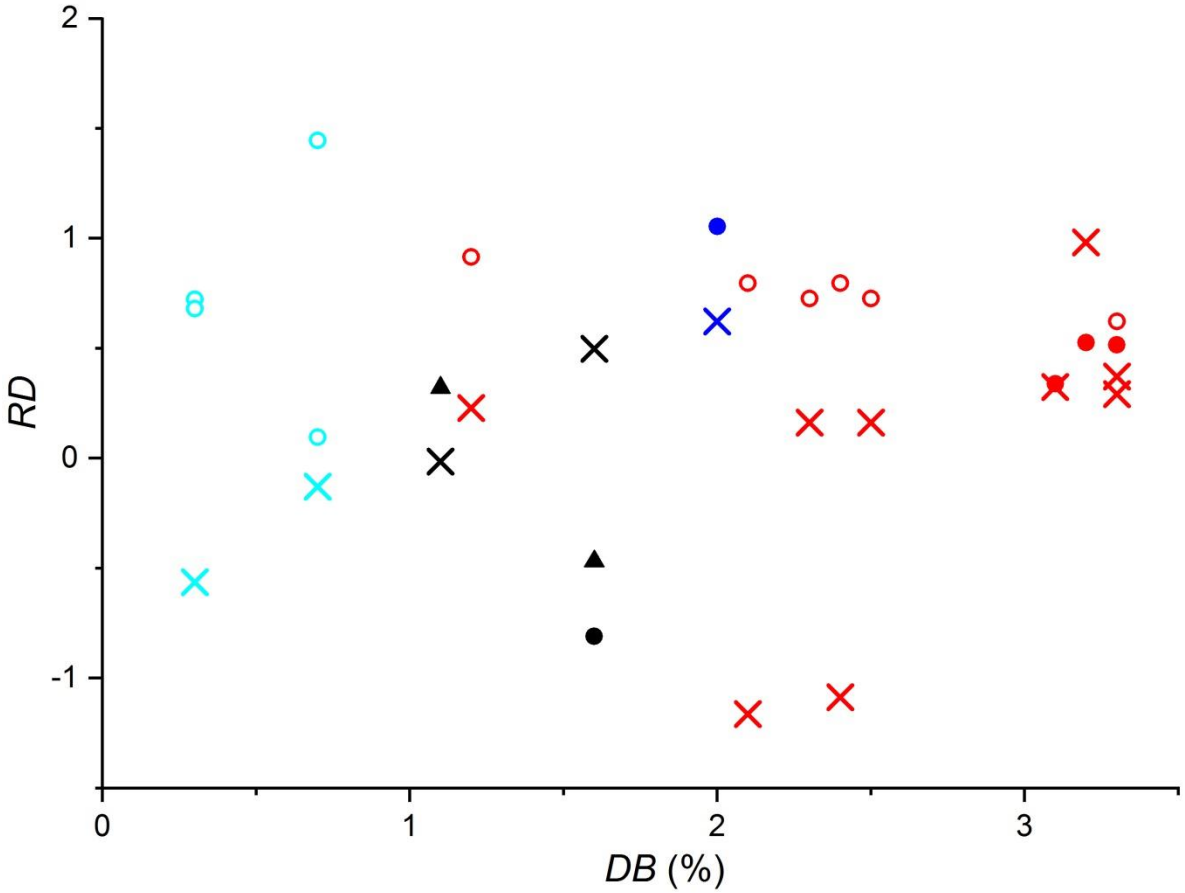

Figure S19. Relative difference (*RD*) between $M_{n(ex)}$ and $M_{n(th)}$ plotted as a function of *DB* (%) for PAAs/PNaAs synthesized in dioxane using ^{13}C (✕) NMR spectroscopy or organic-phase (●) and aqueous-phase (○) SEC, for PAAs/PNaAs synthesized in bulk using ^{1}H (▲) and ^{13}C (✕) NMR spectroscopy or organic-phase SEC (●),for PAAs/PNaAs synthesized in water/ethanol using ^{13}C NMR spectroscopy (✕) or aqueous-phase SEC (○), for PAAs/PNaAs synthesized in water using ^{13}C NMR spectroscopy (✕) or aqueous-phase SEC (○).

Presence of macromonomers

The presence of macromonomers due to β-scission was observed for several PAAs synthesized via NMP at 120 °C (NMP-AA-1, NMP-AA-3 and NMP-AA-4). These signals overlapped with the residual monomer signals (as shown in [2]) which were also observed in all the mentioned samples.

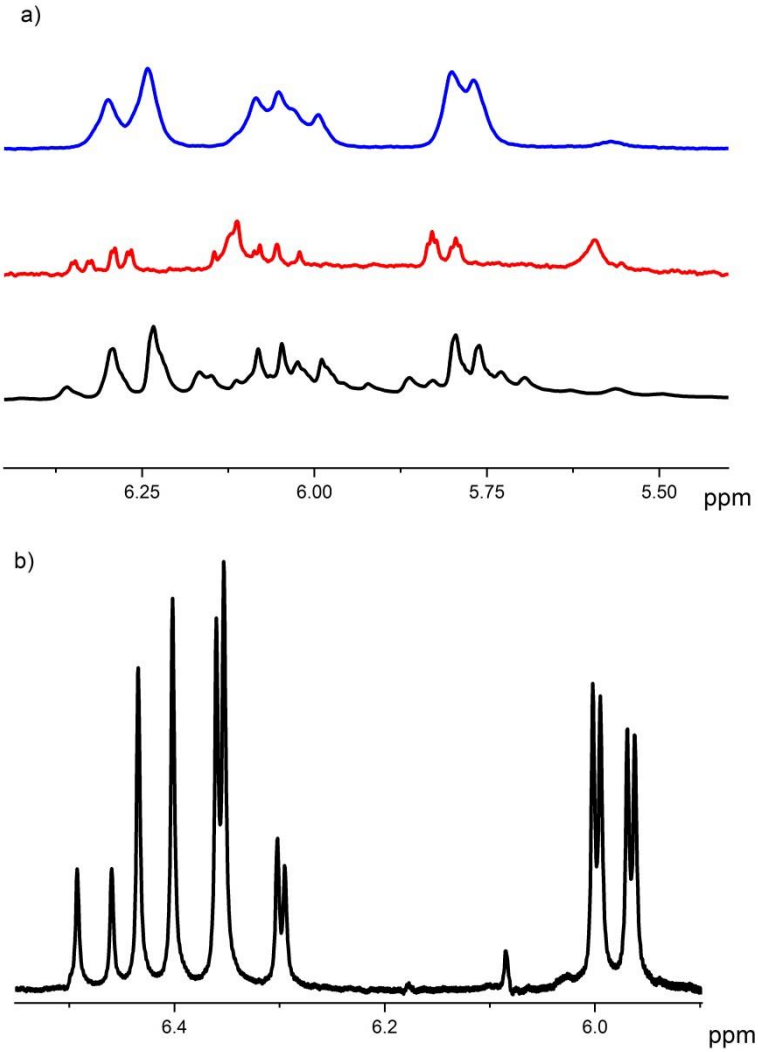

Figure S20. [1]H NMR spectra of a) NMP-AA-1 (black), NMP-AA-3 (red) and NMP-AA-4 (blue) confirming the presence of macromonomers. b) Reference spectrum of the residual monomer[2].

Rate coefficients of intramolecular transfer to polymer

Ratios of the rate coefficient of intramolecular transfer to polymer to the rate coefficient of propagation, k_{bb}/k_p, were estimated using the following equation:[7]

$$DB = \frac{k_{bb} 100 \cdot \ln\left([M]_0 / [M]_e\right)}{k_p \left([M]_0 - [M]_e\right)} \quad \text{(S28)}$$

which can be rearranged into:

$$\frac{k_{bb}}{k_p} = \frac{DB \cdot \left([M]_0 - [M]_e\right)}{100 \cdot \ln\left([M]_0 / [M]_e\right)} \quad \text{(S29)}$$

and where *DB* is the degree of branching, $[M]_0$ is the initial monomer concentration, and $[M]_e$ is the final monomer concentration. The assumptions must be made that every transfer to polymer event leads to branching and that the incidence of the following events may be disregarded: intermolecular chain transfer to polymer, MCR patching, β-scission and termination by disproportionation, as well as monomer consumption via addition to MCR.

k_{bb}/k_p ratios were quantified for samples MADIX-AA-3 to -6, NMP-AA-1, -3, and -4, as well as CVRP-AA-1, using $[M]_0$ given in Table S1, $[M]_e$ determined from $[M]_0$ and conversion from Table S1, and DB given in Table S11. The determined k_{bb}/k_p values are listed in Table S12 and plotted on Figure 3.

Table S12. Ratios of the rate coefficient of intramolecular transfer to polymer to the rate coefficient of propagation, k_{bb}/k_p, for several polymerizations of AA/NaA (see Table S1 for more experimental polymerization parameters). 1000/T is the inverse polymerization temperature.

Experiment code	***1000/T (K^{-1})***	k_{bb}/k_p
NMP-AA-1	2.54	0.848 ± 0.065
NMP-AA-3	2.54	1.110 ± 0.067
NMP-AA-4	2.54	1.080 ± 0.068
NMP-AA-5A	2.54	0.050 ± 0.016
NMP-AA-5 B	2.54	0.031 ± 0013
NMP-AA-6	2.75	0.012 ± 0012
MADIX-AA-1	3.00	0.00243 ± 0.00081
MADIX-AA-2	3.00	0.00276 ± 0.00039
MADIX-AA-3	3.25	0.0115 ± 0.0019
MADIX-AA-4 A	3.00	0.02012 ± 0.00084
MADIX-AA-4 B	3.00	0.01760 ± 0.00084
MADIX-AA-5 A	2.75	0.0193 ± 0.0017
MADIX-AA-5 B	2.75	0.0210 ± 0.0017
MADIX-AA-6	2.61	0.0378 ± 0.0017
CVRP-AA-1 *	2.83	0.0706 ± 0.0054, 0.0308 ± 0.0023

* two values were calculated for this samples for conversions of 0.2 and 0.9.

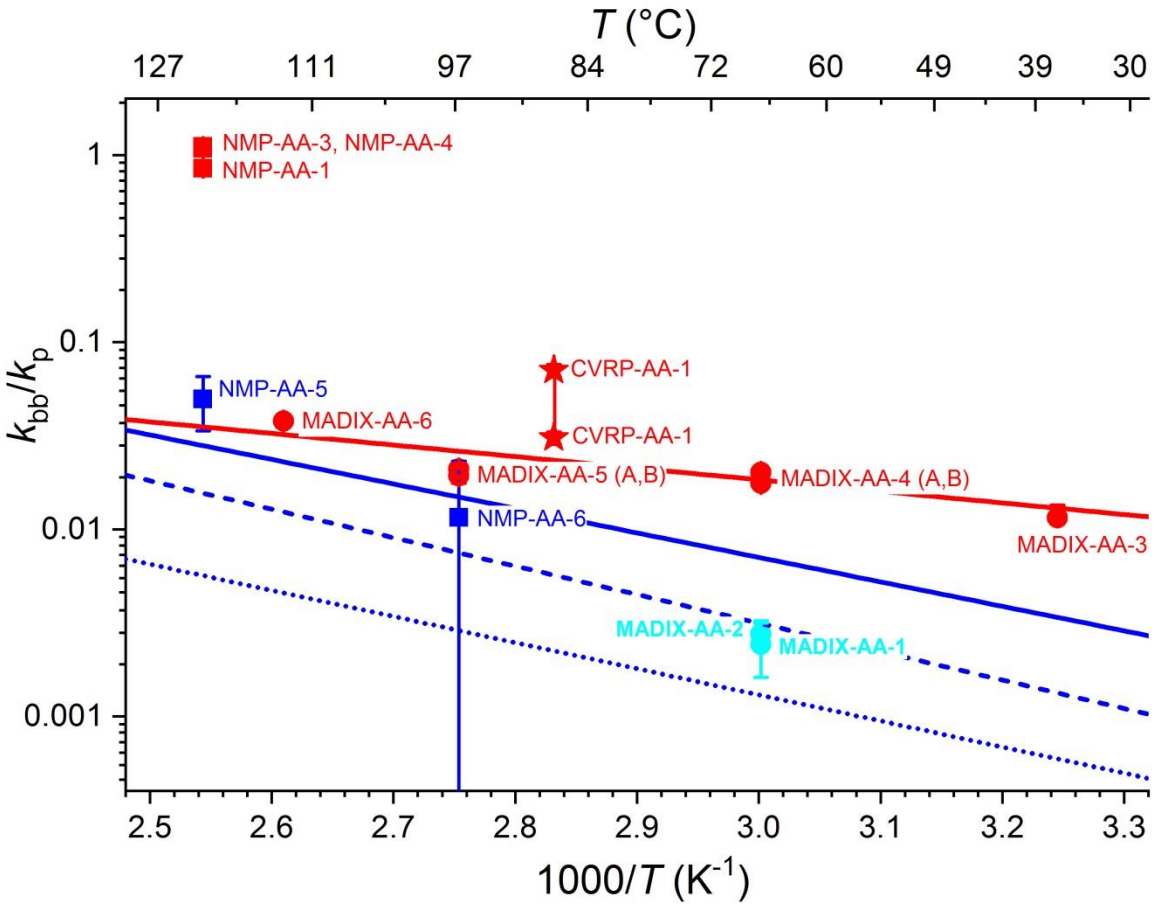

Figure S21. Larger version of Figure 3 with data points labelled with sample codes. The plotted data is also listed in Table S12. Arrhenius plot of k_{bb}/k_p for AA/NaA in dioxane by NMP (■), MADIX (●) and CVRP (★), in toluene with CVRP with CTA (☆), in water with NMP (■), in water/ethanol with MADIX (●).The error bars are based on the precision estimated from the sensitivity of the NMR measurement. — represents the Arrhenius fit for MADIX in 1,4-dioxane-d_8 (ln y = -1425x + 0.28). – – and ····· represent Arrhenius fits from previous studies with CVRP in water: with and without CTA [8] (ln y = -3213x +2.998 and ln y = -3502x +4.747, respectively) and without CTA [3] (solid line, ln y = -3012x + 4.086).

References

1. A. R. Maniego, A. T. Sutton, M. Gaborieau and P. Castignolles, *Macromolecules*, 2017, **50**, 9032–9041.
2. A. R. Maniego, D. Ang, Y. Guillaneuf, C. Lefay, D. Gigmes, J. R. Aldrich-Wright, M. Gaborieau and P. Castignolles, *Anal. Bioanal. Chem.*, 2013, **405**, 9009-9020.
3. N. F. G. Wittenberg, C. Preusser, H. Kattner, M. Stach, I. Lacík, R. A. Hutchinson and M. Buback, *Macromol. React. Eng.*, 2015, **10**, 95-107.
4. R. J. Minari, G. Caceres, P. Mandelli, M. M. Yossen, M. Gonzalez-Sierra, J. R. Vega and L. M. Gugliotta, *Macromol. React. Eng.*, 2011, **5**, 223-231.
5. H. Torii, K. Fujimoto and H. Kawaguchi, *J. Polym. Sci. Pol. Chem.*, 1996, **34**, 1237-1243.
6. N. M. Ahmad, B. Charleux, C. Farcet, C. J. Ferguson, S. G. Gaynor, B. S. Hawkett, F. Heatley, B. Klumperman, D. Konkolewicz, P. A. Lovell, K. Matyjaszewski and R. Venkatesh, *Macromol. Rapid Commun.*, 2009, **30**, 2002-2021.
7. A. N. Nikitin, R. A. Hutchinson, G. A. Kalfas, J. R. Richards and C. Bruni, *Macromol. Theory Simul.*, 2009, **18**, 247-258.
8. J.-B. Lena, A. K. Goroncy, J. J. Thevarajah, A. R. Maniego, G. T. Russell, P. Castignolles and M. Gaborieau, *Polymer*, 2017, **114**, 209-220.